Supporting Information

Fluorescein Analogue Xanthene-9-Carboxylic Acid: A Transition-Metal Free CO Releasing Molecule Activated by Green Light

Lovely Angel Panamparambil Antony,[§] Tomáš Slanina,[§] Peter Šebej, Tomáš Šolomek, and Petr Klán*

Department of Chemistry and Research Centre for Toxic Compounds in the Environment, Faculty of Science, Masaryk University, Kamenice 5, 625 00, Brno, Czech Republic

* klan@sci.muni.cz
[§] These authors contributed equally

Contents

Materials and Methods

The reagents and solvents of the highest purity available were used as purchased, or they were purified/dried using the standard methods when necessary. Synthetic procedures were performed under ambient atmosphere unless stated otherwise. In some cases, the Schlenk techniques were used for working with air- and/or moisture-sensitive chemicals. Oxygen was removed from the solutions by three freeze-pump-thaw cycles or bubbling with inert gas (N_2 or Ar) for at least 15 min.

NMR spectra were recorded on 300 or 500 MHz spectrometers in methanol-d_4, water-d_2, their mixtures, or deuterated 0.1 M phosphate buffers at 30 °C. Buffer solutions were prepared by dissolution of the corresponding amounts of anhydrous Na_3PO_4 in D_2O or $D_2{}^{18}O$ and titrated with aq DCl (2%, v/v) to pH = (7.4 ± 0.1). The fraction of ^{18}O in $D_2{}^{18}O$ was determined by mass spectrometry (~55%). The signals in ^1H and ^{13}C NMR spectra were referenced[1] to the residual peak of a (major) solvent except for D_2O. The deuterated solvents were kept under dry N_2 atmosphere. UV-vis spectra were obtained with matched 0.1 or 1.0 cm quartz cuvettes. Fluorescence was measured on an automated luminescence spectrometer in 1.0 cm quartz fluorescence cuvettes at 26 ± 1 °C; the sample concentration was set to keep the absorbance below 0.1 at λ_{max}; each sample was measured five times and the corrected spectra were averaged. Emission and excitation spectra are normalized and were corrected using standard protocols. Fluorescence quantum yields were determined in 1.0 cm quartz fluorescence cuvettes at 26 ± 1 °C using an integration sphere as the absolute values. For each

sample, the quantum yield was measured five times and the values were averaged. IR spectra of solid samples were obtained on an FT spectrometer using KBr pellets. IR spectra of the gas samples were obtained on a single-beam FT spectrometer in a gas-tight cell with 10 cm optical path and CsF windows; the spectrometer resolution was set to 0.9 cm^{-1}. Exact masses were obtained by a triple quadrupole electrospray ionization mass spectrometer in positive or negative mode coupled with direct inlet or liquid chromatography. Head-space mass spectra were obtained in a splitless mode with the injector temperature of 100 °C at isothermal conditions: the DB5 chromatographic column was kept isothermally at 30 °C, and He was used as a mobile phase; the signal at 10–50 *m*/*z* was recorded. An automated analyzer was used for thermal scanning calorimetry and coupled thermogravimetry: a ~3 mg sample was heated with gradient of 10 K min^{-1} under dry N_2 atmosphere. Released gases were analyzed by a coupled standard gas-phase FT IR spectrometry. Melting points were obtained on a non-calibrated Kofler's hot stage melting point apparatus. Lyophilization was performed at 5 Pa and 20 °C. The solution pH values were always determined using a glass electrode calibrated with certified buffer solutions at pH = 4, 7 and 10. The output spectra of the light sources used were measured with a calibrated portable spectrophotometer. All measurements were conducted at 20 °C, unless stated otherwise.

All calculations were performed in Gaussian 09 suite of programs.[2] The ground state geometries were optimized at the B3LYP/6-31+G(d)/PCM(water). Frequency calculations were performed to check the type of the stationary point found and to provide zero-point vibrational energies (ZPVEs) that were used unscaled to calculate energies at 0 K. Intrinsic reaction path (IRC) calculations were performed to find the connection of optimized transition states with the local potential energy minima. TD-DFT approach was used to describe the excited state energy surfaces. Three functionals (BMK,[3] CAM-B3LYP,[4] M06-HF;[5] 6-31G(d) basis set) that are known to provide a reasonable description of local and charge-transfer (CT) electronic states were used to calculate three lowest excited states. The BMK functional with equilibrium solvation was considered during excited state geometry optimizations. The final energies on the S_1 potential energy surface were not corrected by ZPVEs.

Diethyl (6-Hydroxy-3-oxo-3*H*-xanthen-9-yl)methyl Phosphate•DDQ Complex (2). See Scheme 1 in the main text. This compound was prepared and characterized in our previous work.[6]

6-Hydroxy-3-oxo-3*H*-xanthene-9-carboxylic Acid (1). This procedure was adopted from our previous work,[6] scaled-up and optimized. Diethyl (6-hydroxy-3-oxo-3*H*-xanthen-9-yl)methyl phosphate•DDQ complex (**2**, 73 mg, 0,121 mmol) was dissolved under vigorous stirring for 30 min in aq phosphate buffer (100 mL, *c* = 0.1 M, pH = 7.4). The resulting solution was quantitatively transferred into a large covered Petri-dish (30 cm diameter) in a thin layer (thickness of ~4 mm). The solution was cooled in an ice bath and irradiated using a 400 W broad-band halogen lamp. The reaction progress was monitored by ^{1}H NMR using an identical sample (in D_2O-based buffer) in NMR cuvette irradiated simultaneously. When no starting material was observed (in ~12 h), the solution was collected and acidified with ~5 mL of concentrated trifluoroacetic acid to pH = 2 to precipitate the crude product. This solution was left in dark for 45 min to let the solid formed precipitate. The suspension was decanted and filtered on a small Büchner funnel (3 cm diameter). The solid was washed with aq trifluoroacetic acid (1%, v/v), collected and dried by lyophilization to give a pure product. Yield: 15.0 mg (48%). Brown solid. Mp: >250 °C (decomposition). ^{1}H NMR (500 MHz, D_2O-based 0.1 M aq phosphate buffer, pH = 7.4): δ (ppm) 6.68 (s, 2H), 6.86 (d, 2H, J = 8.9 Hz), 7.65 (d, 2H, J = 8.9 Hz) (Figure S4). ^{13}C NMR (126 MHz, D_2O-based 0.1 M aq

phosphate buffer at pH = 7.4): δ (ppm) 103.8, 108.5, 123.1, 130.8, 153.6, 159.3, 171.6, 179.5 (Figure S5). FTIR (KBr, cm^{-1}): 3437 (br), 1608, 1504, 1454, 1306, 1269, 1211, 1178, 1117, 1036, 954, 852. UV-vis (0.1 M phosphate aq buffer at pH = 7.4, $c = 1.4 \times 10^{-5}$ mol dm^{-3}): λ_{max} (ε) = 262 (4.23), 488 (4.27) nm (log dm^3 mol^{-1} cm^{-1}) (Table S1, Figure 1 and S11). Fluorescence (0.1 M aq phosphate buffer at pH = 7.4, A (λ_{max} (excitation)) $\leq$ 0.1): λ_{max} (emission) = 532 nm (Table S1, Figure 1 and S11). HRMS (TOF MS ES^+): calcd for $C_{14}H_9O_5$ [M + H^+] 257.0444, found 257.0452 (Figure S9). HRMS (TOF MS ES^+): calcd for $C_{14}H_9{}^{16}O_3{}^{18}O_2$ [M + H^+] 261.0529, found 261.0551 (Figure S10).

Note: No effect of oxygen on the course of the reaction or on the distribution of photoproducts was observed. The maximum chemical yield was ~50% which supports the role of DDQ as a sole oxidant: one eq of DDQ oxidizes 0.5 eq of released alcohol to the carboxylic acid.[6]

Table S1. Spectroscopic Properties of **1**

solvent	absorption[d]		emission	
	λ_{max} / nm	log ε / mol dm^{-3} cm^{-1}	λ_{max} / nm	Φ_f[e]
H_2O, pH = 7.4[a]	488	4.3	532	0.39 ± 0.03
H_2O, pH = 1.0[b]	433	4.1	549	0.027 ± 0.003
CH_3OH[c]	485	4.0	540	0.52 ± 0.06

[a] 0.1 M Phosphate aq buffer at the given pH. [b] 0.1 M aq HCl; all pH values were determined using a calibrated glass electrode. [c] A commercial non-dried solvent. [d] The λ_{max} refers to the highest absorption band observed in the visible part of the spectrum; log ε refers to this λ_{max}. [e] The average and the standard deviation in a set of five independent measurements.

Determination of p$K_{a,c}$ of 1

A freshly prepared solution of **1** in aq phosphate buffer (3 mL, I = 0.1 M, pH ~ 7.4) was transferred into a matched 1.0 cm quartz cuvette and its UV-vis absorption spectrum was obtained. The corresponding amounts of aq HCl (typically 10 μL; 0.1 M, 0.01 M or 0.001 M, I = 0.1 M, adjusted by NaCl) were repeatedly added to this solution, while pH and UV-vis absorption spectra were measured after each addition. All these data were processed using a software for single value decomposition analysis to obtain the three expected acid-base equilibria (p$K_{a,c}$ = 6.39 ± 0.02, 5.08 ± 0.07 and 2.96 ± 0.02) among four acid-base forms (**1a-d**; Scheme 2, Figure S15; the molar absorption coefficients are not calculated for **1c**, **d** because the compounds start to precipitate slowly at a low pH).

Irradiation Experiments

Irradiation in UV Cuvettes (a General Procedure). A solution of **1** ($c = 1.34 \times 10^{-4}$ M) in the given solvent (3 mL) in a matched 1.0 cm quartz cuvette was irradiated with a home-made light source equipped with 32 LEDs emitting at λ_{max} = 503 ± 15 nm (the bandwidth at half height = 30 nm; its spectrum is shown in Figure S16); the reaction progress was simultaneously monitored by UV-vis spectrometry using a diode-array spectrophotometer.

Irradiation in NMR Tubes (a General Procedure). Alternatively, a solution of **1** ($c = 6.7 \times 10^{-3}$ M) in D_2O-based aq phosphate buffer (0.5 mL, I = 0.1 M, pH = 7.4) in an NMR tube was irradiated with a 500 W broadband halogen lamp while both the NMR tube and the lamp in a protective glass coat were immersed in an ethanol bath (T ~ 0 °C). The reaction progress was followed by ^{1}H NMR until no starting material was observable.

An undetermined product with λ_{max} of 430 nm (Figure S21) was formed in aq solution at pH = 9.5 in which **1a** is present exclusively. On the other hand, the starting compound precipitated at pH = 2.5, at which the **1d**/**1c** ratio is ~3:1 (Figure S14). The photochemistry thus could not be studied.

3,6-Dihydroxy-9*H*-xanthen-9-one (3). This photoproduct was isolated as the only non-gaseous photoproduct upon irradiation of **1** in water, aqueous buffer solution at pH 7.4 and 5.73, methanol or a MeOH/H_2O (9:1, v/v) mixture. It was characterized by ^{1}H and ^{13}C NMR, and HRMS previously.[6]

Quantum Yield Determination

A solution of diethyl (6-hydroxy-3-oxo-3*H*-xanthen-9-yl)methyl phosphate•DDQ complex (**2**, $c = 1.11 \times 10^{-3}$ M in aq phosphate buffer, $I = 0.1$ M, pH = 7.4; $\Phi_{disapp.} = 0.017 \pm 0.003$)[6] was used as an actinometer. Both **2** and **1** ($c = 1.34 \times 10^{-3}$ M in aq phosphate buffer, $I = 0.1$ M, pH = 7.4) were irradiated in matched 0.1 cm quartz cuvettes using light pulses (425.6 Hz frequency, pulse length ≤ 150 fs and energy ~4.0 ± 0.1 mW) from a Ti:Sa laser coupled to a noncollinear optical parametric amplifier (NOPA), with wavelength set to 489 ± 7 nm (bandwidth at half height of ~15 nm). The UV-vis spectra of both actinometer (**2**) and **1** solutions were measured repeatedly. The data were processed using a single value decomposition software assuming the A→B kinetics of the first order rate.

Trapping and Determination of Released CO

Preparation of Stock Solutions of the Hemoglobin Forms (MetHb, Hb, HbO_2, HbCO). Bovine blood hemoglobin was obtained from a commercial source as a lyophilized powder. It was dissolved (5.0 mg) in phosphate aqueous buffer (25 mL, $I = 0.1$ M, pH = 7.4). The solution was filtered through a cotton pad to remove non-dissolved particles of denatured proteins and transferred to a UV cuvette. In the commercially available bovine hemoglobin sample, hemoglobin was determined to be almost exclusively in the form of methemoglobin (MetHb, uncomplexed Fe^{III}) by comparison of the measured UV-vis spectrum with that published before.[7] Other forms, possibly present as minor impurities (Hb, HbO_2), were oxidized to MetHb by careful purging of the UV cuvette with oxygen for 2 hours. The absolute concentration of methemoglobin in the solution ($c = 2.3 \times 10^{-5}$ M) was determined by UV-vis spectrometry using the published data (ε(560 nm) = 3.98 dm^3 mmol^{-1} cm^{-1}).[7] This hemoglobin solution was used fresh or stored in dark for less than 24 h before application. The photostability of this solution was also tested: a freshly prepared solution ($c \sim 2.3 \times 10^{-5}$ mol dm^{-3}, A(405 nm) = 0.8) in aq phosphate buffer (3.0 mL, $I = 0.1$ M, pH = 7.4) was transferred into a matched 1.0 cm quartz cuvette, purged with dry nitrogen (to avoid interference with atmospheric oxygen) for 30 min, and subsequently irradiated with a home-made light source equipped with 32 LEDs emitting at $\lambda_{max} = 503 \pm 15$ nm for 17.5 h (Figure S16). Methemoglobin was stable against photobleaching (<2% over 17.5 h of irradiation under these conditions as determined by change of the absorbance at 405 nm; Figure S19).

Deoxyhemoglobin (Hb, uncomplexed Fe^{II}) was prepared by addition of a small excess of sodium dithionite solution into the UV cuvette with the solution of bovine hemoglobin purged by nitrogen. As $Na_2S_2O_4$ strongly absorbs below 320 nm[8] and interferes with the absorption of Hb, the amount of added sodium dithionite should be smaller than 1.1 eq. A fresh solution of sodium dithionite (1.0 mg, 5.7 μmol) in phosphate aqueous buffer (25 mL, $I = 0.1$ M, pH = 7.4) was prepared before each experiment because sodium dithionite is rapidly oxidized in aqueous solutions losing its reducing power.[9] Hb is susceptible to oxidation by traces of oxygen in the system, thus careful purging of the solution with dry nitrogen was found to be essential before and after addition of sodium dithionite.

Oxyhemoglobin (HbO_2, Fe^{II} complexed with O_2) was prepared from Hb by purging its aq solution with oxygen for 5 min. HbO_2 is unstable in the solution and is oxidized exhaustively to methemoglobin within 60 min.

Carboxyhemoglobin (HbCO, Fe^{II} complexed with CO) was prepared from Hb by purging its aq solution with carbon monoxide (for preparation *vide infra*) for 10 min. Alternatively, HbCO was also obtained by addition of saturated CO (aq) solution to an aq MetHb solution. In both cases, the resulting HbCO was stable in aerated aqueous solutions for at least 4 h. Hemoglobin derivatives could be easily distinguished from each other by their characteristic absorption bands in the visible part of the spectrum (Table S2 and Figure S17).

Table S2. Absorption properties of hemoglobin derivatives[a]

	λ_{max} / nm	ε (560 nm) / $dm^3\ mol^{-1}\ cm^{-1}$	A (rel., at λ_{max})
MetHb	406	3980	1.00
Hb	429	13010	0.65
HbO_2	414	8680	0.44
HbCO	419	12180	0.44

[a] Known molar absorption coefficients (ε) at 560 nm,[7] the relative absorbances A (at λ_{max}) of the solutions of MetHb, Hb, HbO_2, and HbCO in 0.1 M aq phosphate buffer at pH = 7.4, prepared from MetHb solutions ($c = 2.3 \times 10^{-5}$ mol dm^{-3}).

Preparation of CO as an Analytical Standard and its Qualitative Determination. Carbon monoxide was generated by dehydration of formic acid by sulfuric acid. Formic acid (20 mL, >98%) was added dropwise to aq sulfuric acid (98%, 100 mL) in a two-necked 250 mL flask equipped with a magnetic stirrer. After 2 min of stirring at 25 °C, gaseous CO started to evolve and was led by a PE tubing through a Dreschel bottle filled with aq sodium hydroxide (10 M). The pressure of CO in the apparatus was regulated by a three-way valve attached to the end of the tubing. The composition of the generated gas was determined by head-space MS analysis and gas phase IR. The head-space glass vial sealed with a PTFE cap was purged by CO generated from the apparatus for 20 min.

Determination of CO Released from 1. A solution of 6-hydroxy-3-oxo-3*H*-xanthene-9-carboxylic acid (**1**, $c = 1.34 \times 10^{-4}$ mol dm^{-3}, A(489 nm) = 1.5) in aq phosphate buffer (3.0 mL, I = 0.1 M, pH = 7.4) in matched 1.0 cm fluorescence cuvette sealed with a PTFE cap was purged by nitrogen for 10 min. The sample was irradiated with a home-made light source equipped with 32 LEDs emitting at λ_{max} = 503 ± 15 nm for 18 h until ~50% conversion was reached (UV-vis spectrophotometry). The sample was transferred by a syringe to a solution of Hb (*vide supra*) in a different fluorescence cuvette sealed with a PTFE cap. The immediate appearance of the peak of carboxyhemoglobin (HbCO) was monitored by UV-vis spectrometry (Figure S20).

The release of CO was also determined by its complexation with deoxyhemoglobin (Hb) by direct **in situ** irradiation (the same irradiation source as described above; 4 h) of a mixture of **1** (402 nmol, $c = 1.34 \times 10^{-4}$ mol dm^{-3}, A(489 nm) = 1.5) and Hb (69 nmol, $c = 2.3 \times 10^{-5}$ mol dm^{-3}, A(405 nm) = 0.85) in aq phosphate buffer (3.0 mL, c = 0.1 M, pH = 7.4) in a fluorescence cuvette sealed with a PTFE cap. The appearance of a signal of HbCO was monitored by UV-vis spectrophotometry (Figure 2). A stability of both **1** and Hb solutions in dark was followed spectrophotometrically: about 10% disappearance of **1** was found presumably due to its reduction by $Na_2S_2O_4$ present in the solution (Figure S19).

Dark Chemistry of 1

In addition to photoinduced extrusion of CO from **1** (Schemes 3 and S1, pathway a), thermal decomposition of 6-hydroxy-3-oxo-3*H*-xanthene-9-carboxylic acid **1** gives carbon dioxide. DSC/TG analysis with a coupled IR measurement showed CO_2 as the only observable gaseous byproduct released at 250–270 °C (Figure S25, Scheme S1, pathway b), which corresponds to the observed mp (>250°C; decomposition).

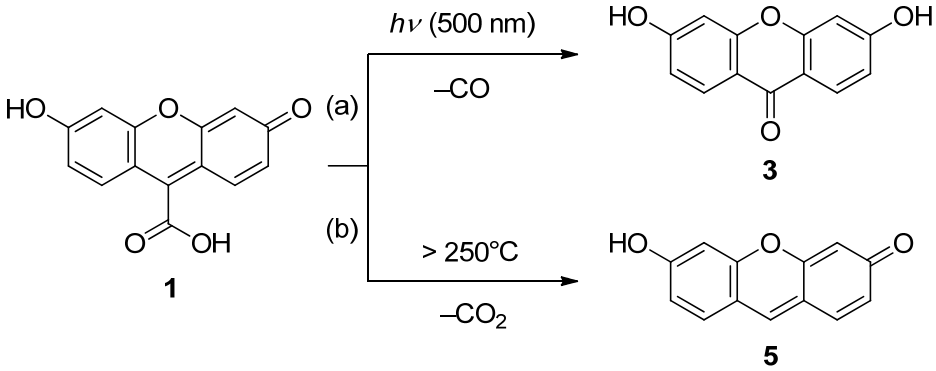

Scheme S1. Photochemical and thermal release of gaseous carbon oxides from **1**

Quantum Chemical Calculations

Table S3. TD-DFT transitions of the dianion form **1a**

functional	excitation energy		oscillator strength	excitation type[a]
	eV	λ (nm)		
BMK	3.1061	399.16	0.8905	local (ππ*)
	3.8881	318.88	0.0000	local (nπ*)
	3.9397	314.70	0.0190	local (ππ*) + CT
CAM-B3LYP	3.1082	398.89	0.8997	local (ππ*)
	4.0558	305.69	0.0291	local (ππ*) + CT
	4.0937	302.87	0.0000	local (nπ*)
M06HF	3.0012	413.12	1.0259	local (ππ*)
	4.1074	301.86	0.0000	local (nπ*)
	4.1425	299.30	0.0000	local (nπ*)

[a] Local transition within the chromophore or CT transition involving the carboxylate group and the xanthene moiety.

Table S4. TD-DFT transitions of the monoanion form **1b**

functional	excitation energy		oscillator strength	excitation type[a]
	eV	λ (nm)		
BMK	3.3076	374.85	0.6363	local (ππ*)
	3.6187	342.62	0.0001	local (nπ*) + CT
	3.7563	330.07	0.0022	local (nπ*) + CT
CAM-B3LYP	3.3313	372.18	0.6703	local (ππ*)

	3.8055	325.80	0.0003	local (nπ*) + CT
	3.8641	320.86	0.0020	local (nπ*) + CT
M06HF	3.4362	360.81	0.8351	local (ππ*)
	3.6216	342.34	0.0000	local (nπ*)
	4.6233	268.17	0.0004	CT

[a] Local transition within the chromophore or CT transition involving the carboxylate group.

Table S5. TD-DFT transitions of the neutral form **1c**.

functional	excitation energy		oscillator strength	excitation type[a]
	eV	λ (nm)		
BMK	3.2043	386.93	0.0029	CT
	3.4173	362.81	0.1649	local (ππ*) + CT
	3.5237	351.86	0.1331	CT
CAM-B3LYP	3.2976	375.99	0.0031	CT
	3.4772	356.57	0.2408	local (ππ*) + CT
	3.5258	351.64	0.1414	CT
M06HF	3.6828	336.65	0.7887	local (ππ*)
	3.8741	320.04	0.0008	CT
	4.1065	301.92	0.0538	local (ππ*)

[a] Local transition within the chromophore or CT transition involving the carboxylate group.

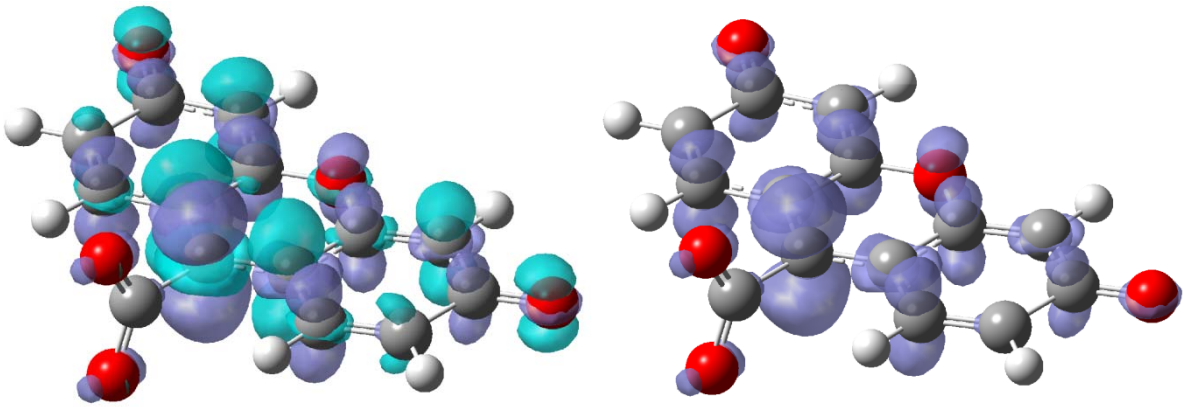

Figure S1. An electron density difference map obtained by subtracting the ground state electron density from the lowest singlet excited state electron density. The violet color represents a positive density difference, i.e., space with building-up of the electron density upon excitation, while the blue-green color represents the electron density depletion. Only the positive part is depicted on the right.

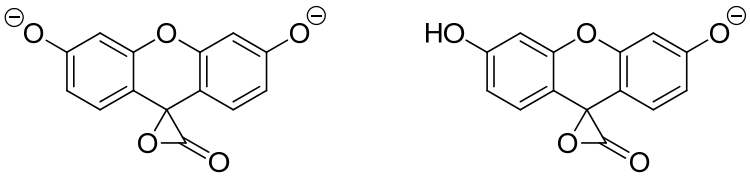

Figure S2. Energy minima of **4** localized on the S_1 potential energy surface using TD-BMK/6-31G(d)/PCM(water) method. Energies relative to the S_1 potential energy minima of **1** in its respective protonation form are shown.

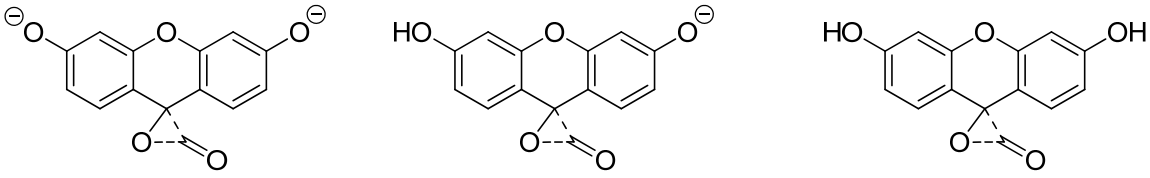

Figure S3. Decarbonylation transition states of various protonation forms of **1** in the ground electronic state and their corresponding energies obtained at B3LYP/6-31+G(d)/PCM(water) level of theory.

Figure S4. ^{1}H NMR (500 MHz): 6-Hydroxy-3-oxo-3*H*-xanthene-9-carboxylic acid (**1**; in D_2O-based 0.1 M aq phosphate buffer at pH = 7.4)

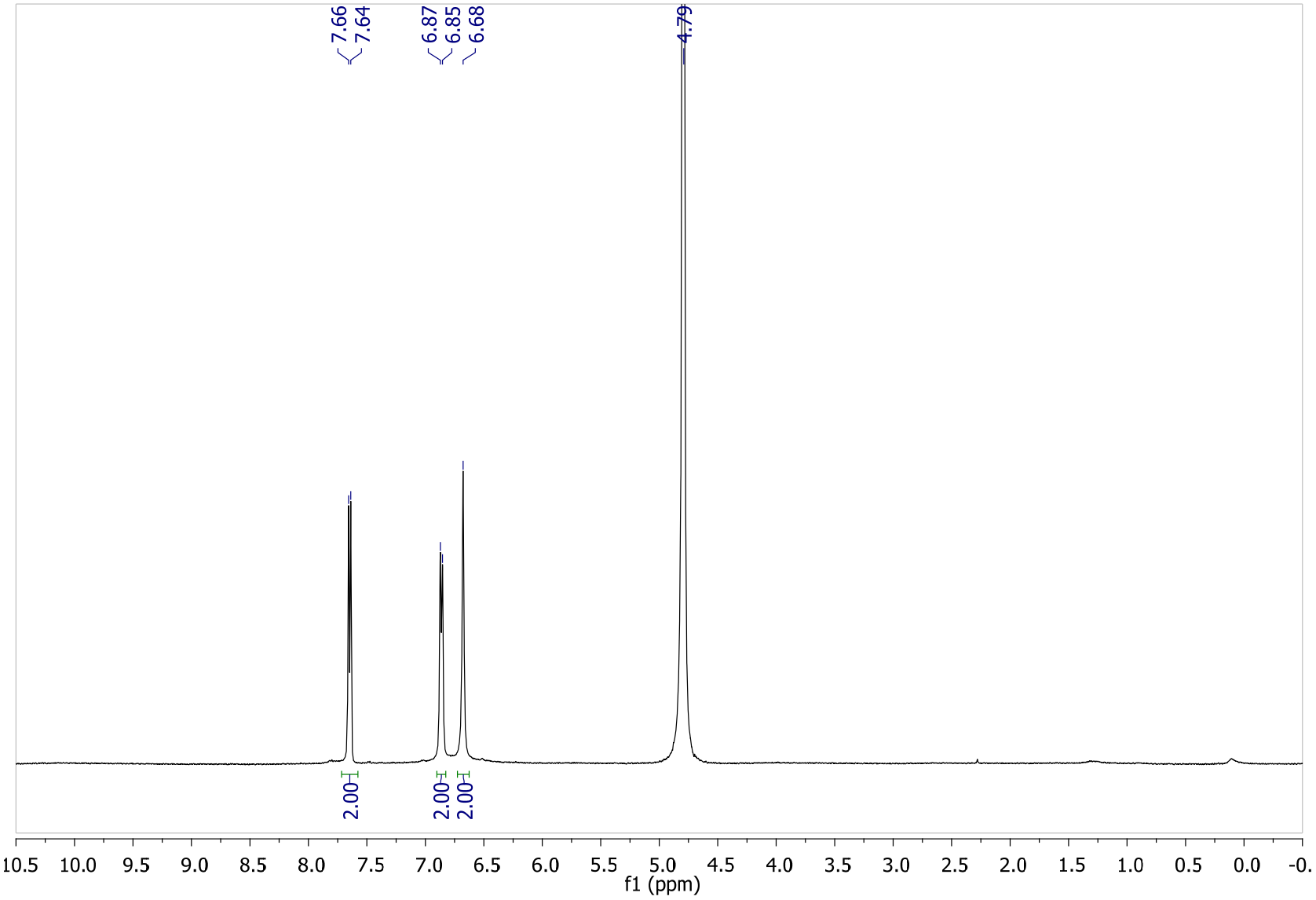

Figure S5. ^{13}C NMR (126 MHz): 6-Hydroxy-3-oxo-3*H*-xanthene-9-carboxylic acid (**1**; in D_2O-based 0.1 M aq phosphate buffer at pH = 7.4)

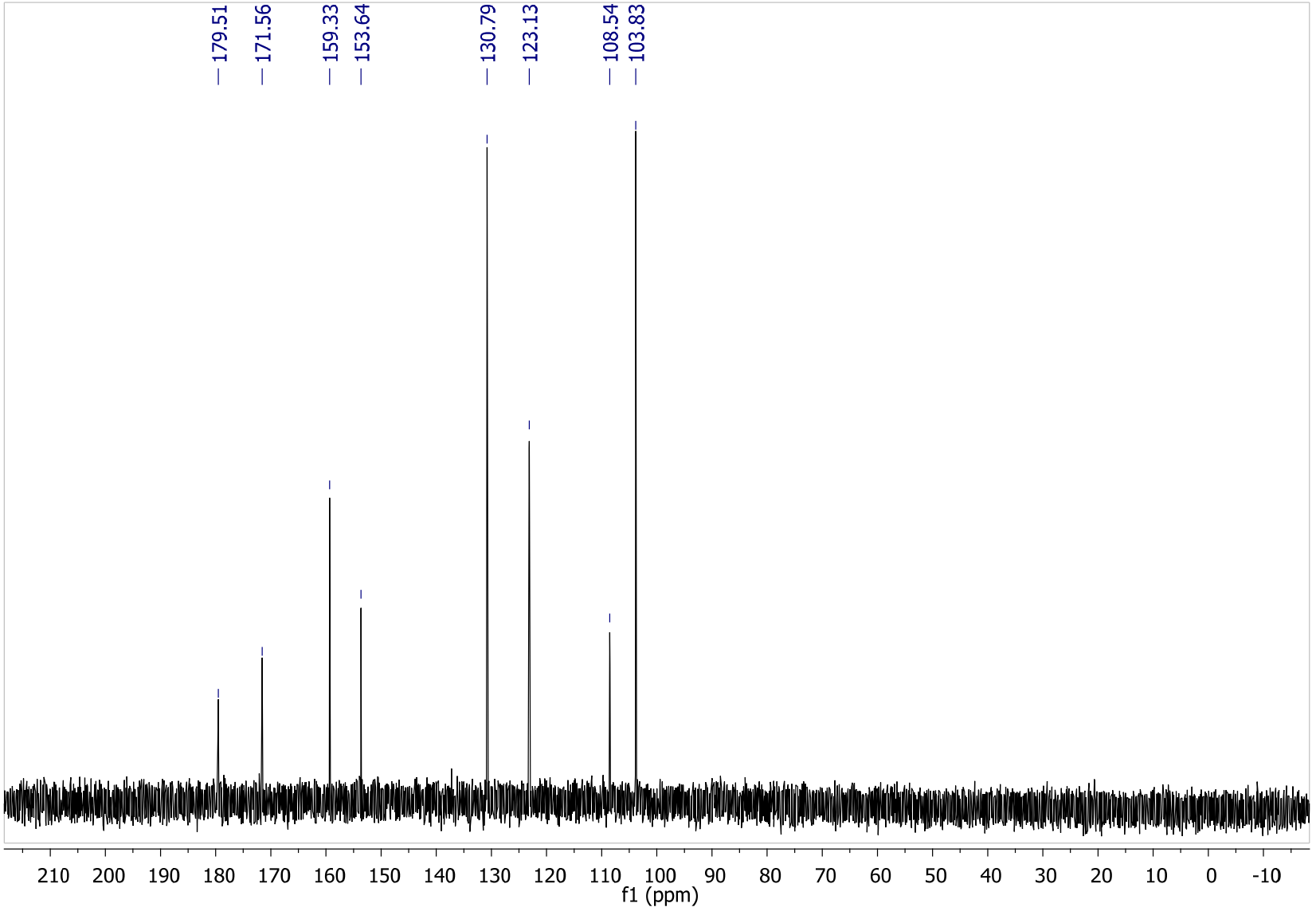

Figure S6. ^{1}H–^{1}H COSY NMR (500 MHz): 6-Hydroxy-3-oxo-3*H*-xanthene-9-carboxylic acid (**1**; in D_2O-based 0.1 M aq phosphate buffer at pH = 7.4)

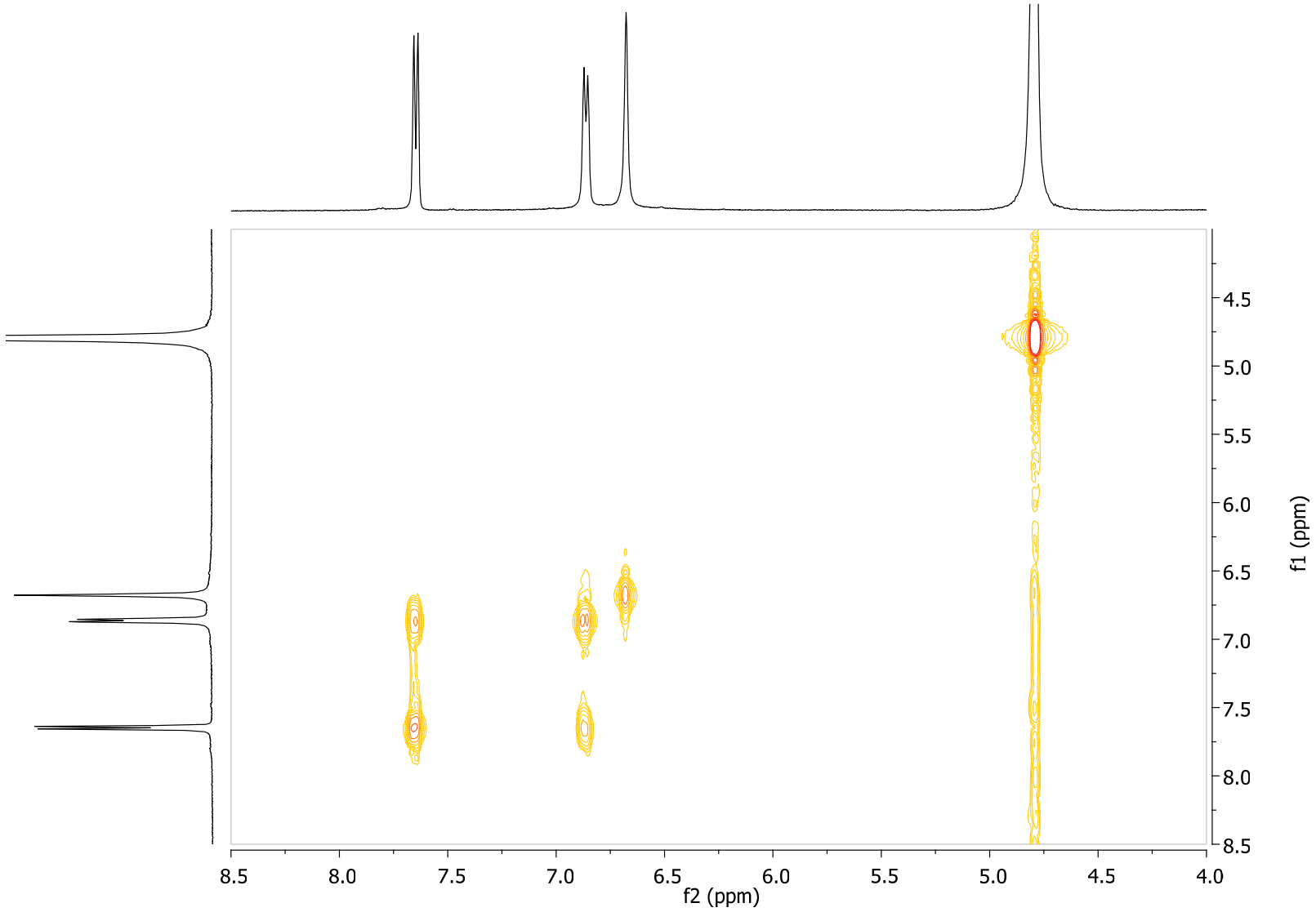

Figure S7. ^{1}H–^{13}C HSQC NMR (500 MHz): 6-Hydroxy-3-oxo-3*H*-xanthene-9-carboxylic acid (**1**; in D_2O-based 0.1 M aq phosphate buffer at pH = 7.4)

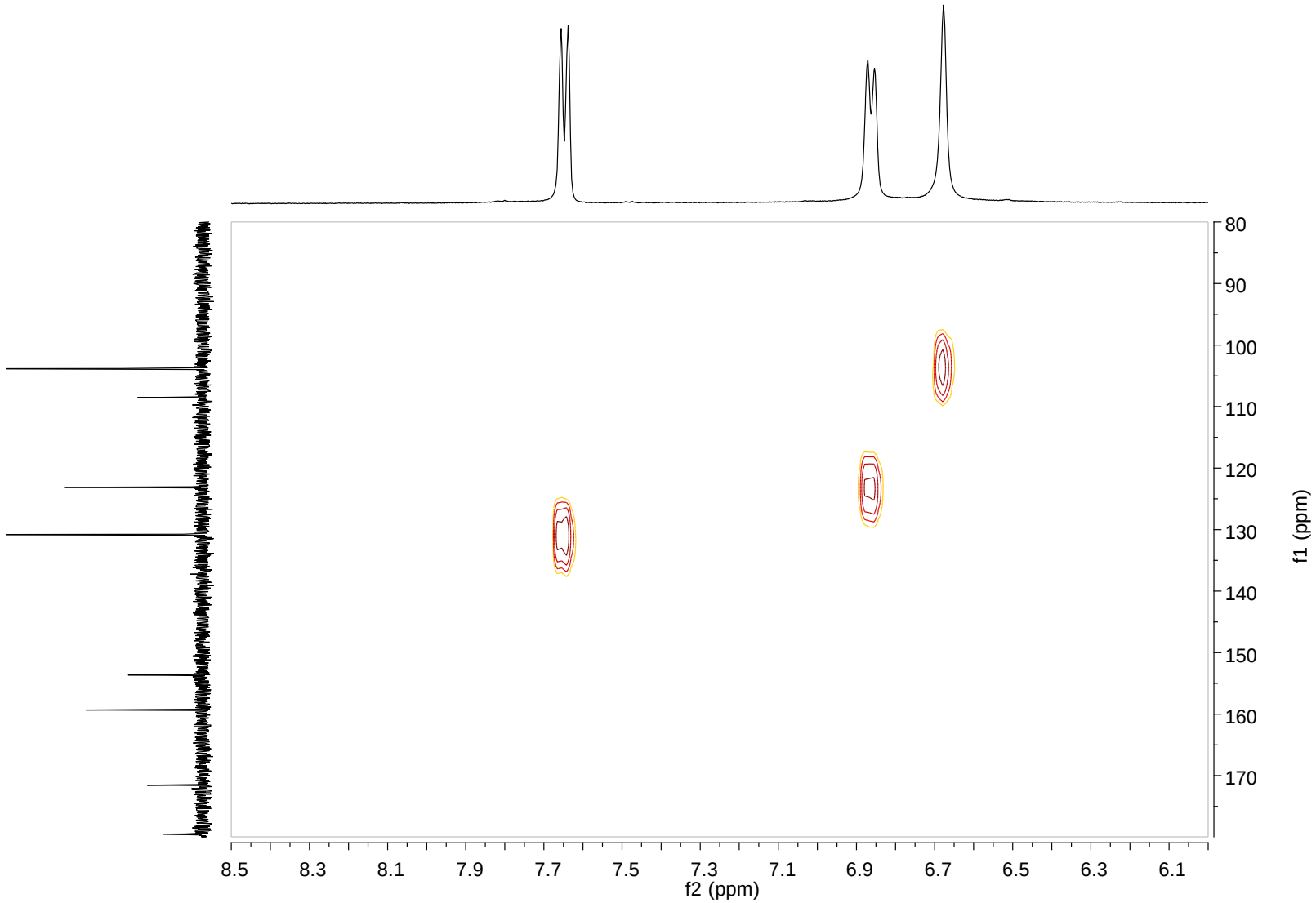

Figure S8. ^{1}H–^{13}C HMBC NMR (500 MHz): 6-Hydroxy-3-oxo-3*H*-xanthene-9-carboxylic acid (**1**; in D_2O-based 0.1 M aq phosphate buffer at pH = 7.4)

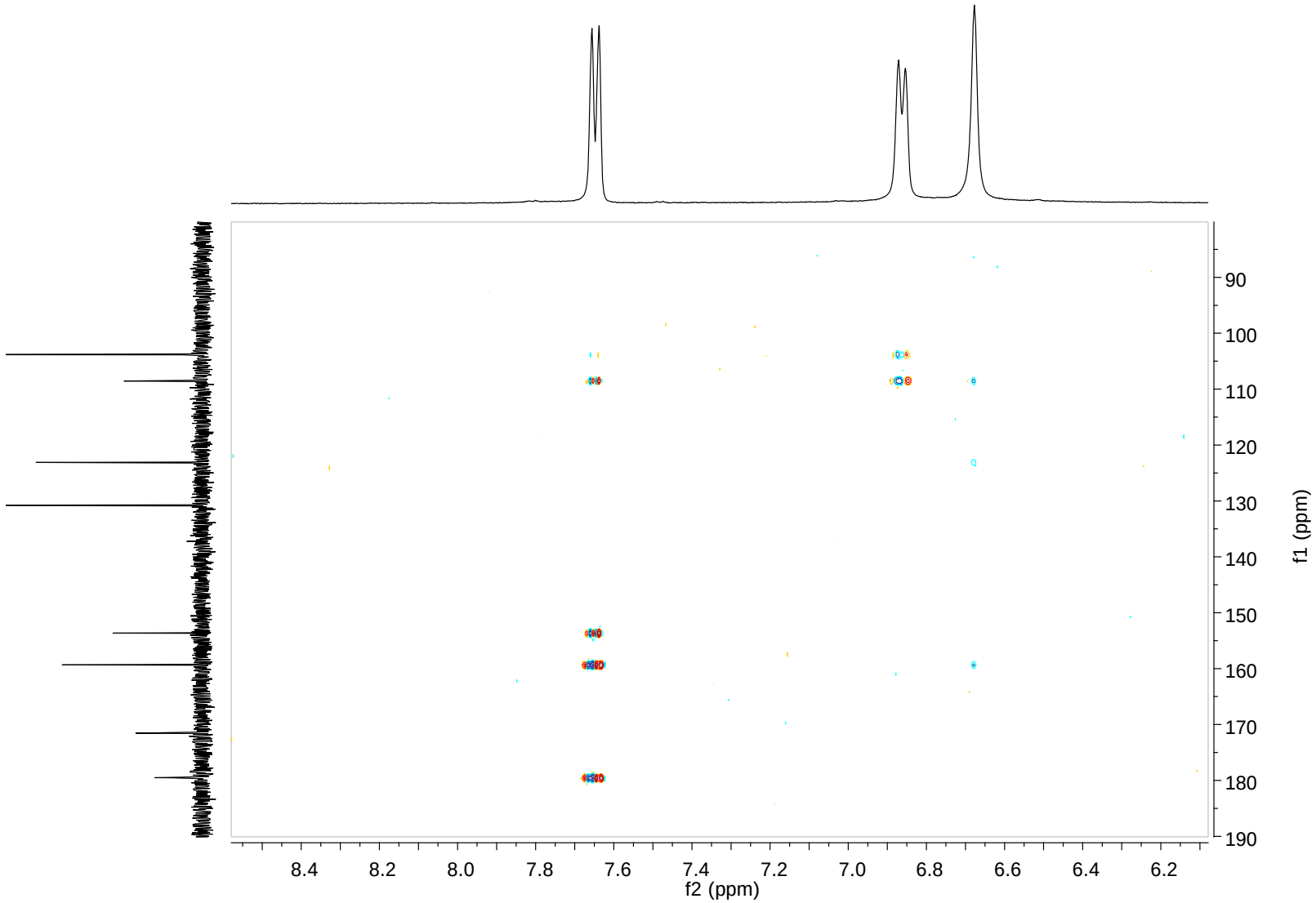

Figure S9. HRMS (ES+): 6-Hydroxy-3-oxo-3*H*-xanthene-9-carboxylic acid (**1**)

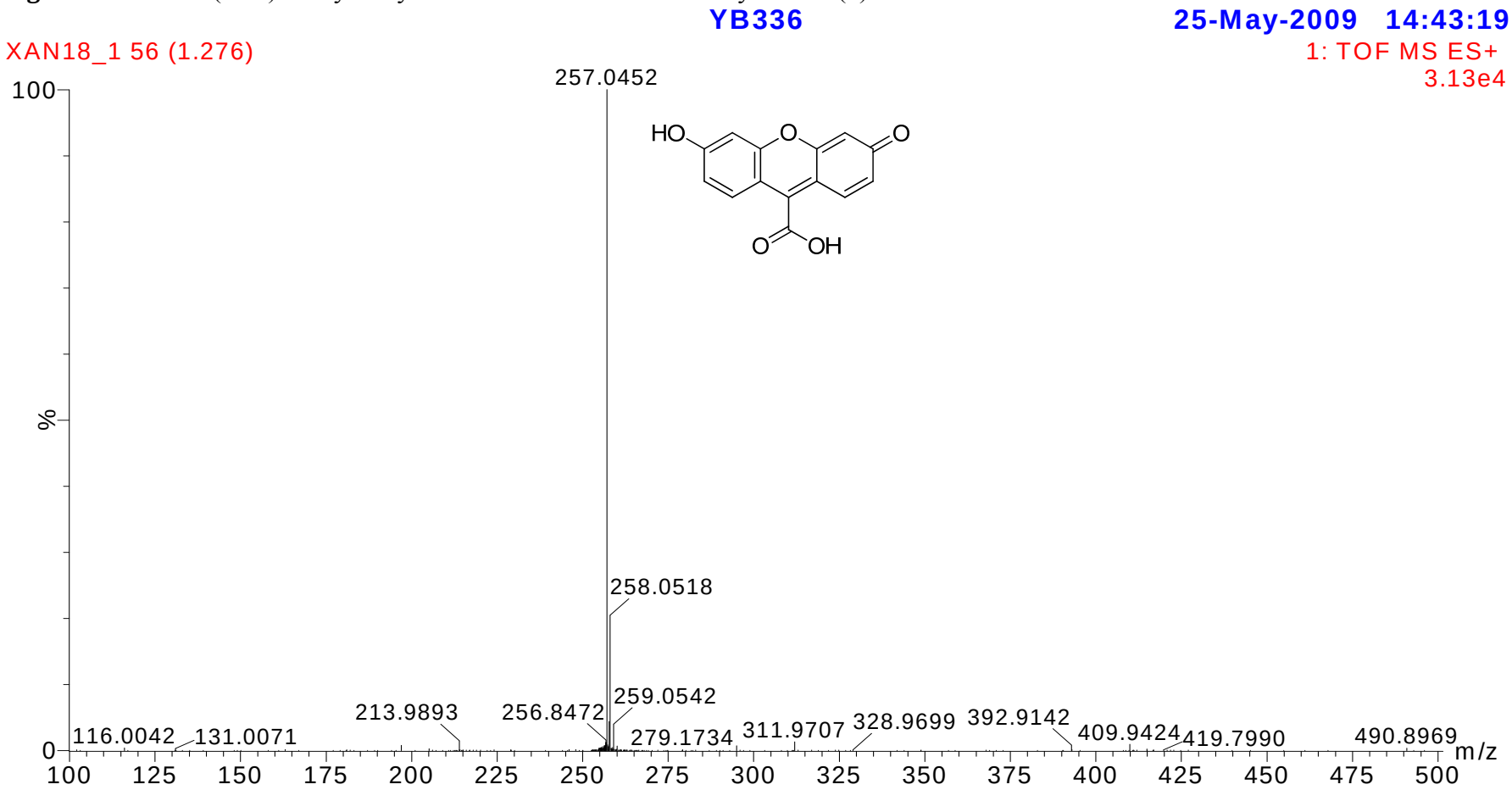

Figure S10. HRMS (ES+): 6-Hydroxy-3-oxo-3*H*-xanthene-9-carboxylic acid (**1**)

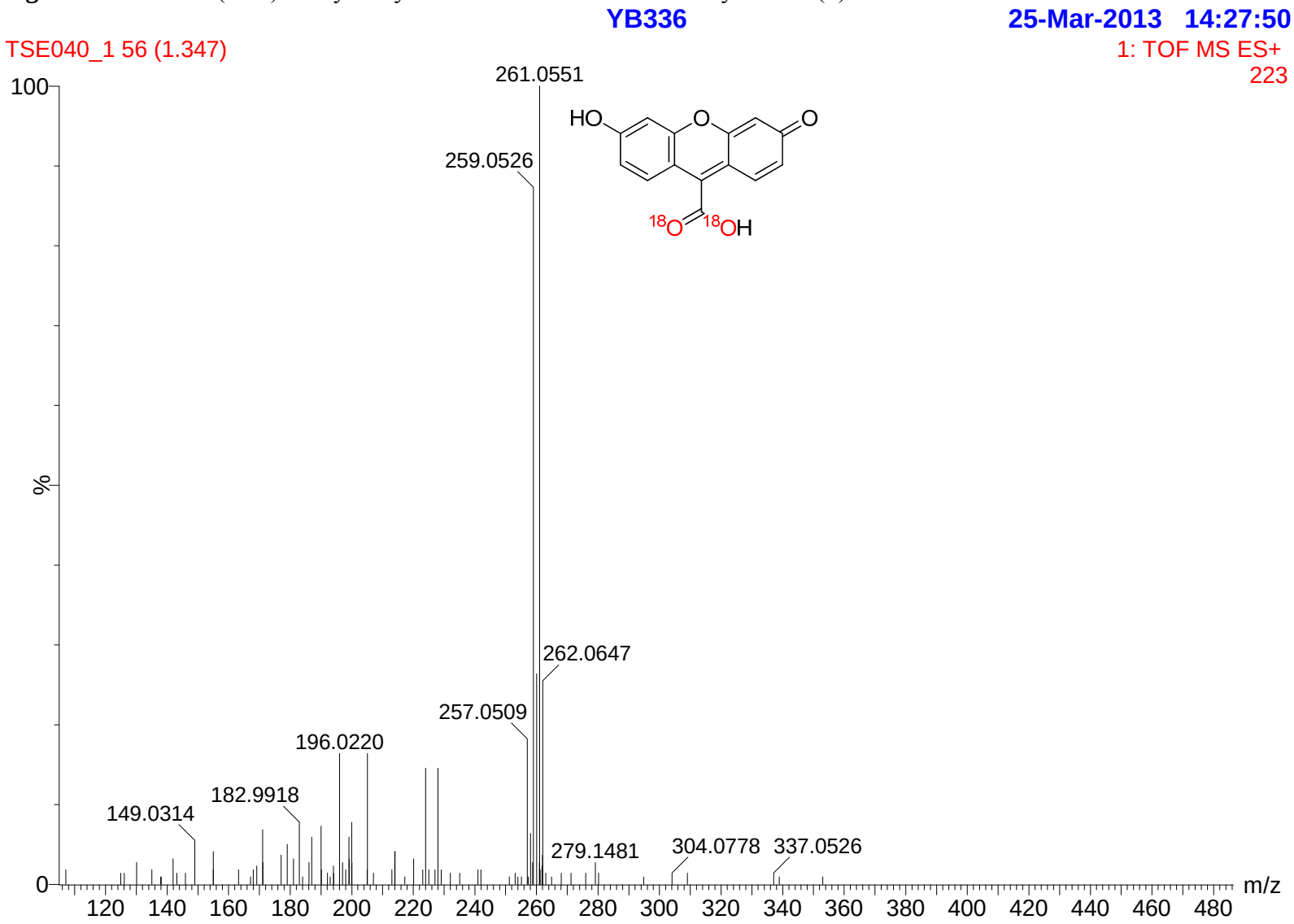

Figure S11. UV-vis and normalized fluorescence spectra (0.1 M aq phosphate buffer at pH = 7.4, $c \sim 1 \times 10^{-5}$ M): 6-Hydroxy-3-oxo-3*H*-xanthene-9-carboxylic acid (**1**)

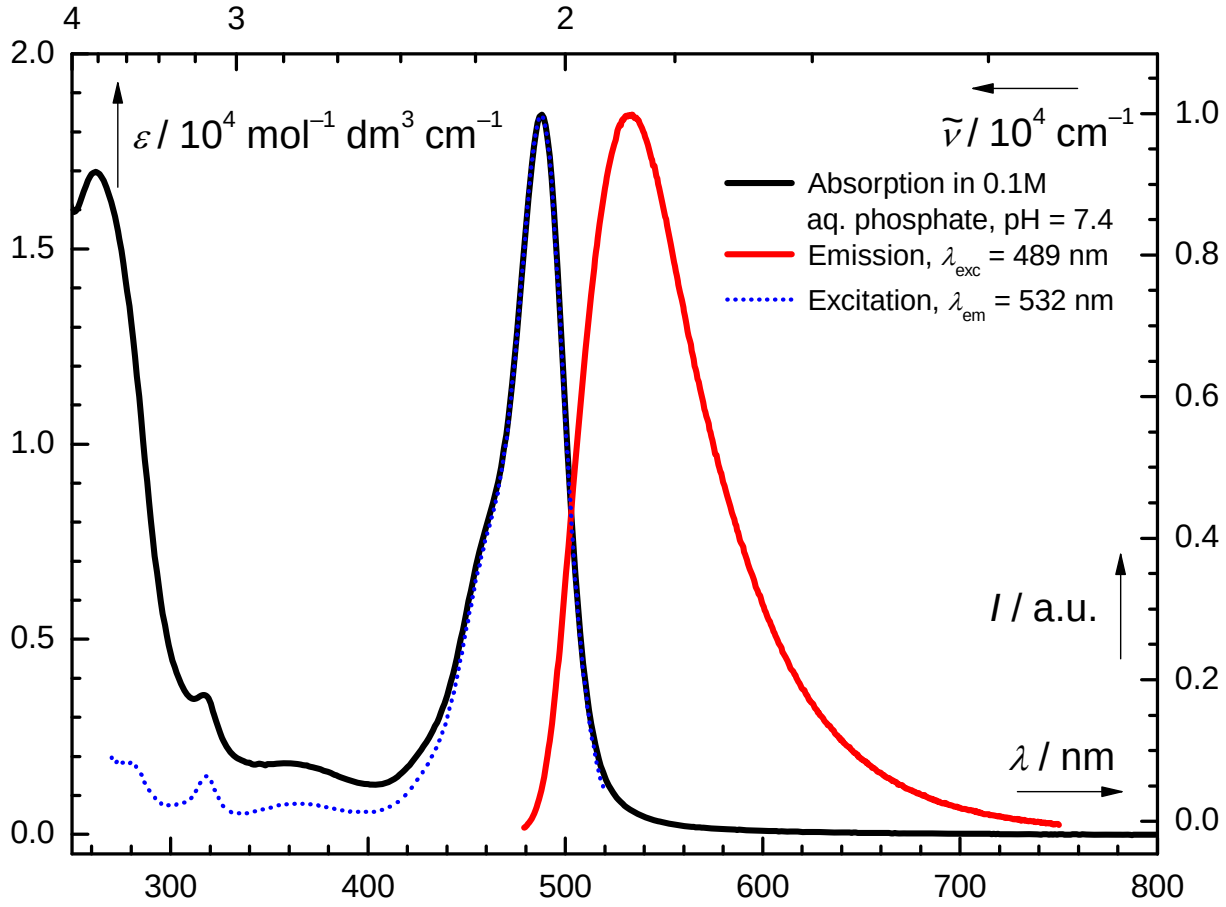

Figure S12. UV-vis and normalized fluorescence spectra (0.1 M aq HCl, $c \sim 1 \times 10^{-5}$ M; a fresh solution): 6-Hydroxy-3-oxo-3*H*-xanthene-9-carboxylic acid (**1**)

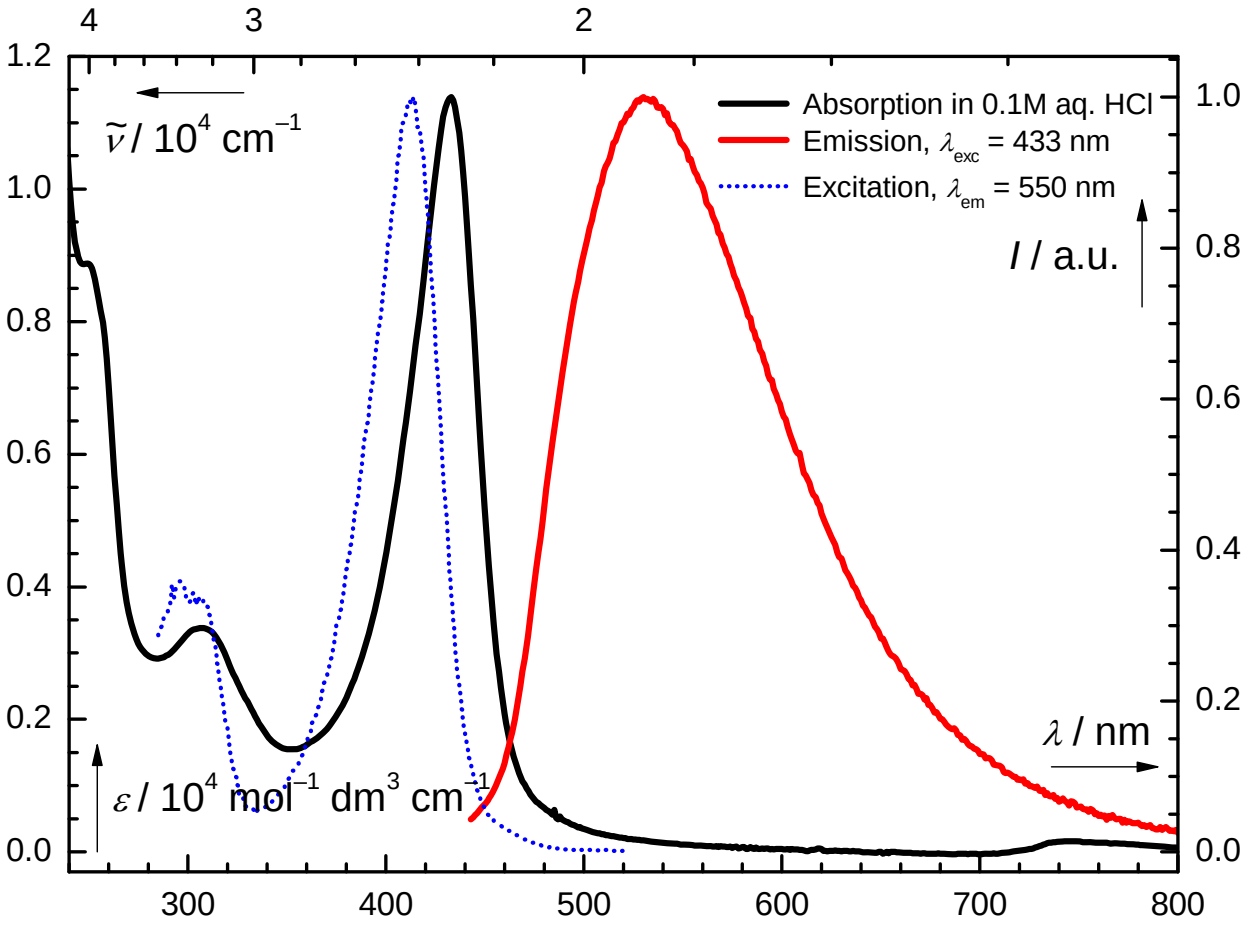

Figure S13. UV-vis and normalized fluorescence spectra (CH_3OH, $c \sim 1 \times 10^{-5}$ M): 6-Hydroxy-3-oxo-3*H*-xanthene-9-carboxylic acid (**1**)

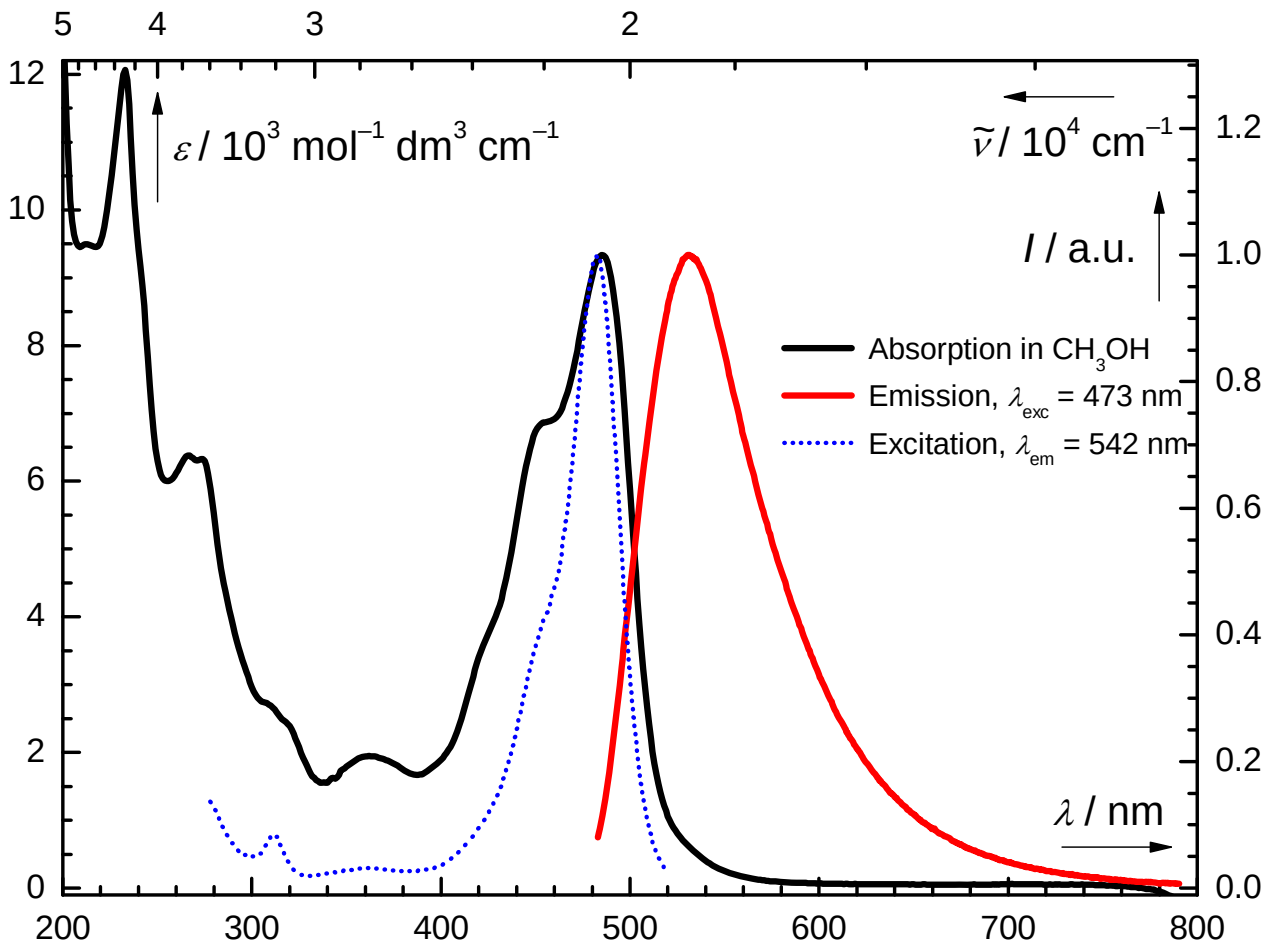

Figure S14. pH dependent speciation (aqueous solution, $I \sim 0.1$ M): 6-Hydroxy-3-oxo-3*H*-xanthene-9-carboxylic acid (**1**) (see Scheme 2 for the structures of **1a-d**)

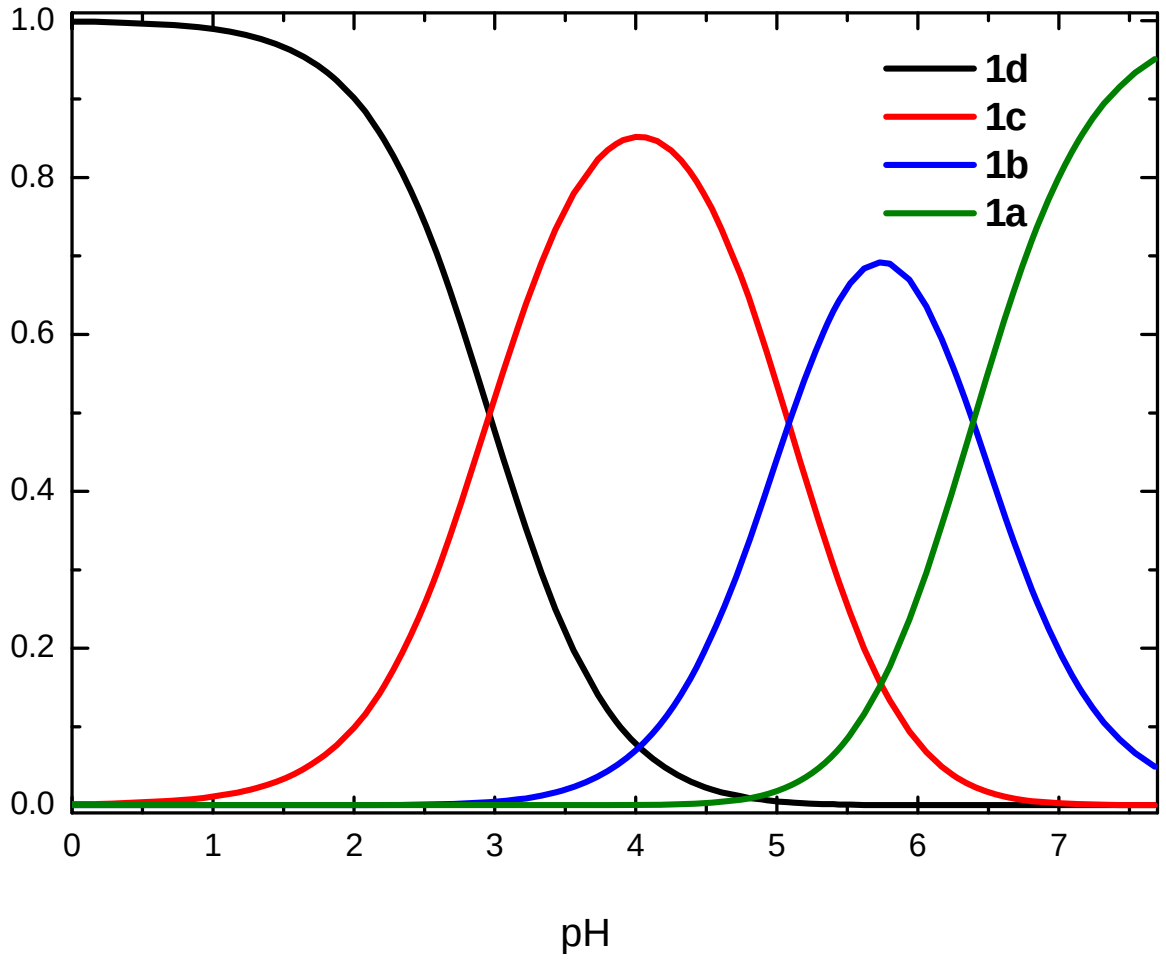

Figure S15. UV-vis spectra (aqueous solution, $I \sim 0.1$ M) of various forms of 6-hydroxy-3-oxo-3*H*-xanthene-9-carboxylic acid (**1**; see Scheme 2 for the structures of **1a-d**). The y-axis has arbitrary units in the case of **1c**, **d**.

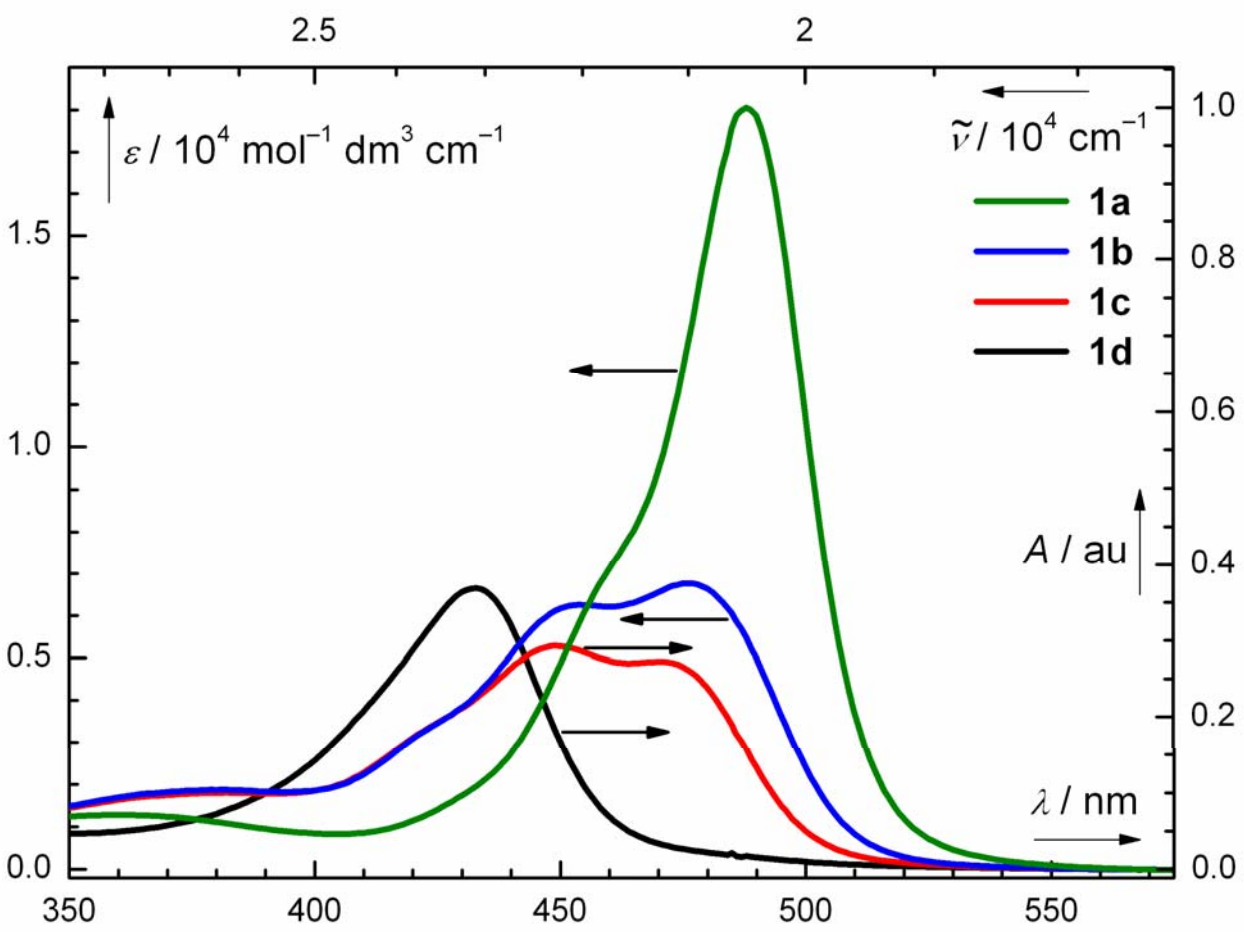

Figure S16. Normalized output spectrum of a home-made light source equipped with 32 light-emitting LEDs (λ_{max} = 503 ± 15 nm).

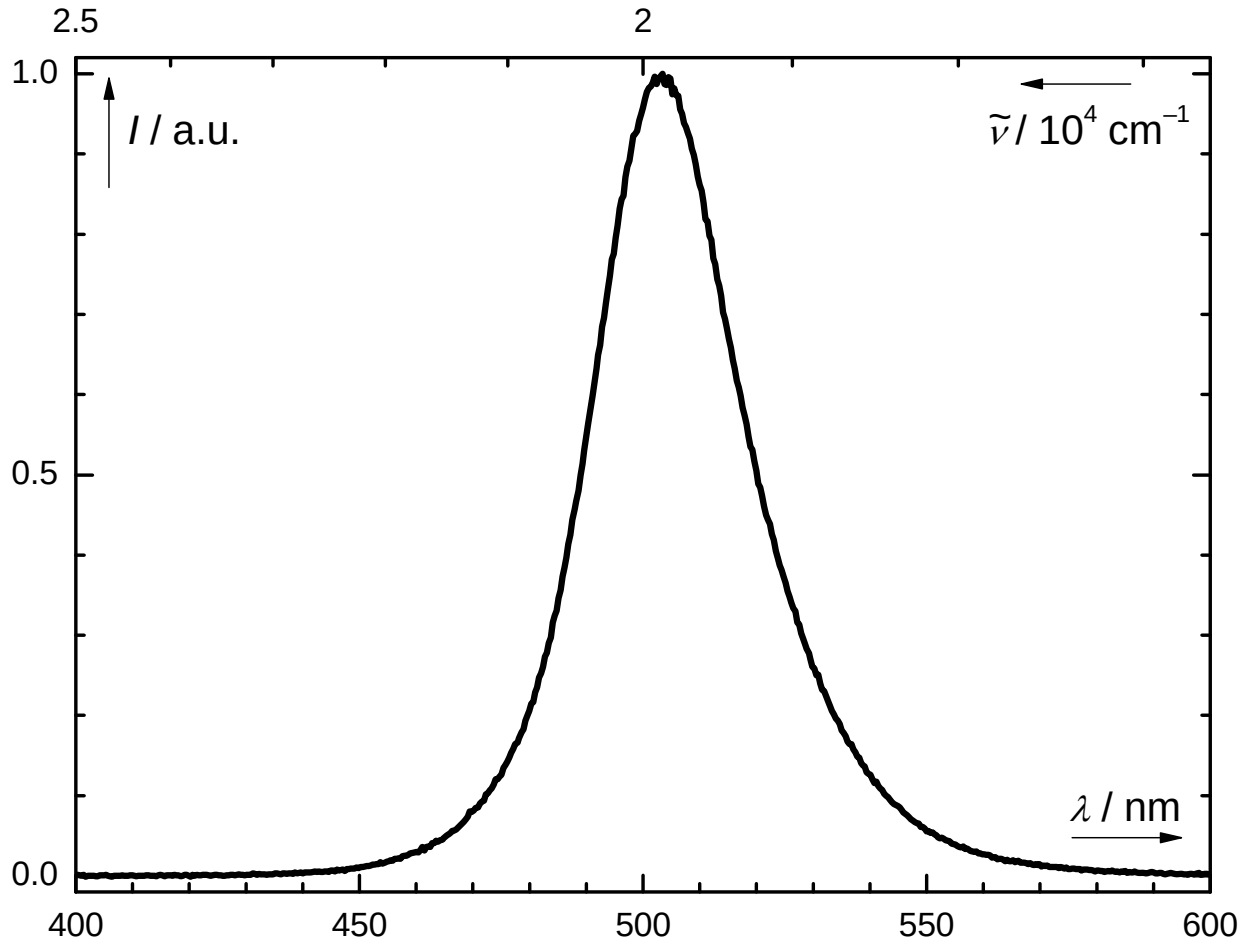

Figure S17. UV-vis (aq phosphate buffer, I ~ 0.1 M, pH = 7.4): hemoglobin (MetHb: uncomplexed, Fe^{III}; Hb: uncomplexed, Fe^{II}; HbO_2: complexed with O_2, Fe^{II} and HbCO: complexed with CO, Fe^{II}; for more details see page S4)

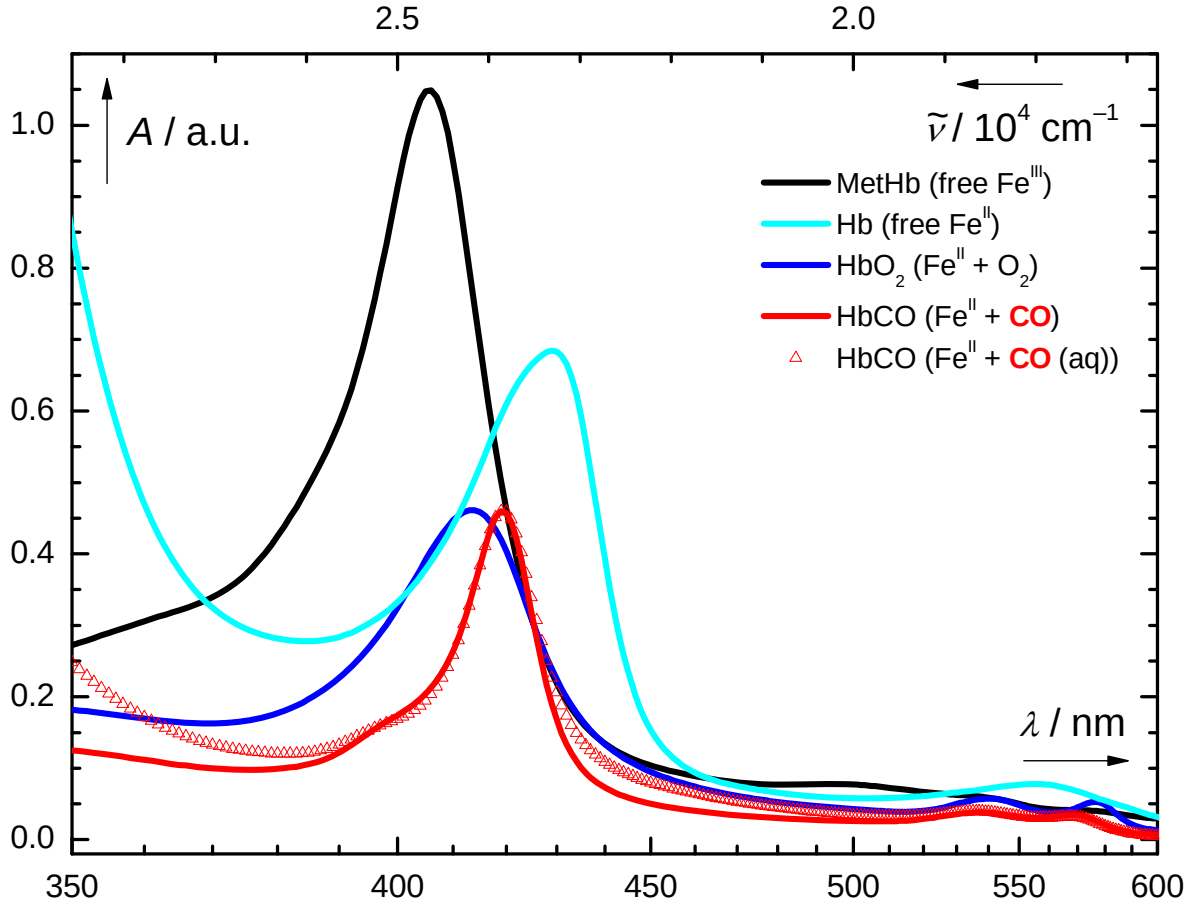

Figure S18. UV-vis spectra (aq phosphate buffer, $I \sim 0.1$ M, pH = 7.4, aerated): MetHb. The sample of MetHb ($c = 2.3 \times 10^{-5}$ mol dm^{-3}, A(405 nm) = 0.8) in a matched 1.0 cm cuvette was irradiated at $\lambda_{max} = 503 \pm 15$ nm for 17.5 hours (the initial spectrum is black, the final is red).

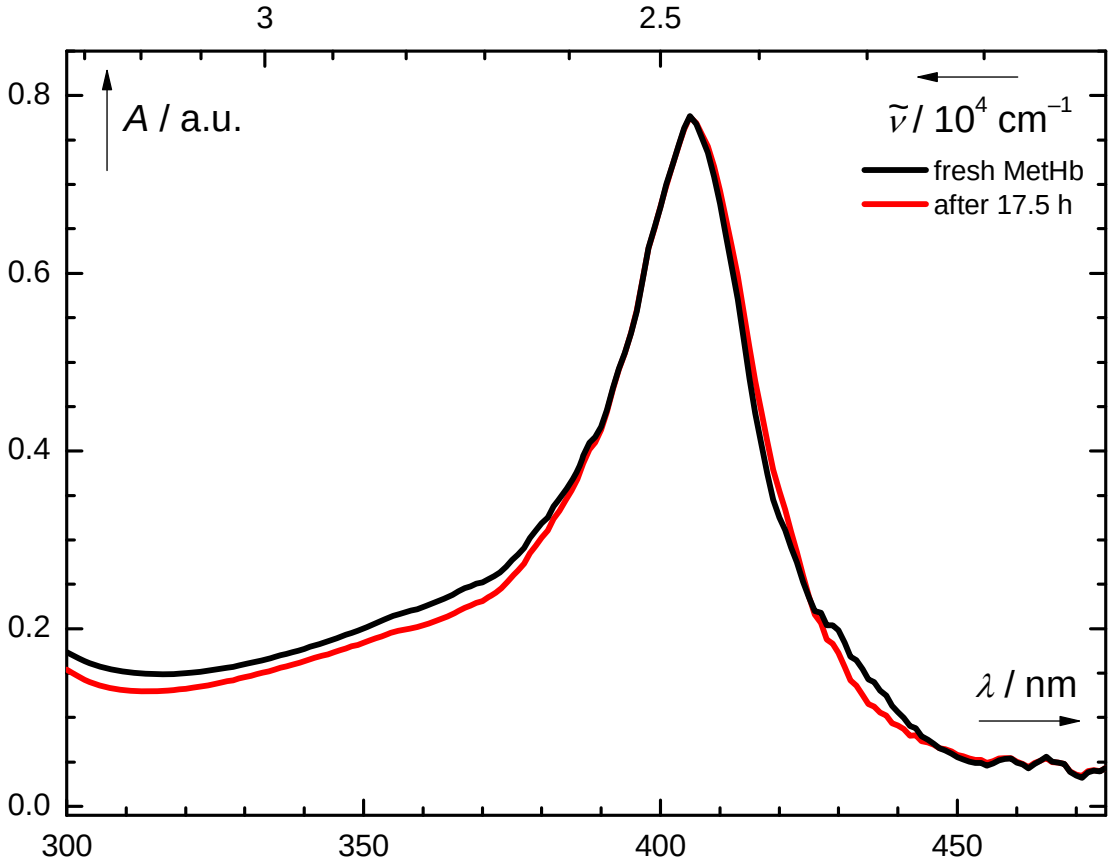

Figure S19. UV-vis (aq phosphate buffer, $I \sim 0.1$ M, pH = 7.4, purged with N_2): Hb and **1** (black line: fresh solution; red line: a solution kept in dark for 90 min)

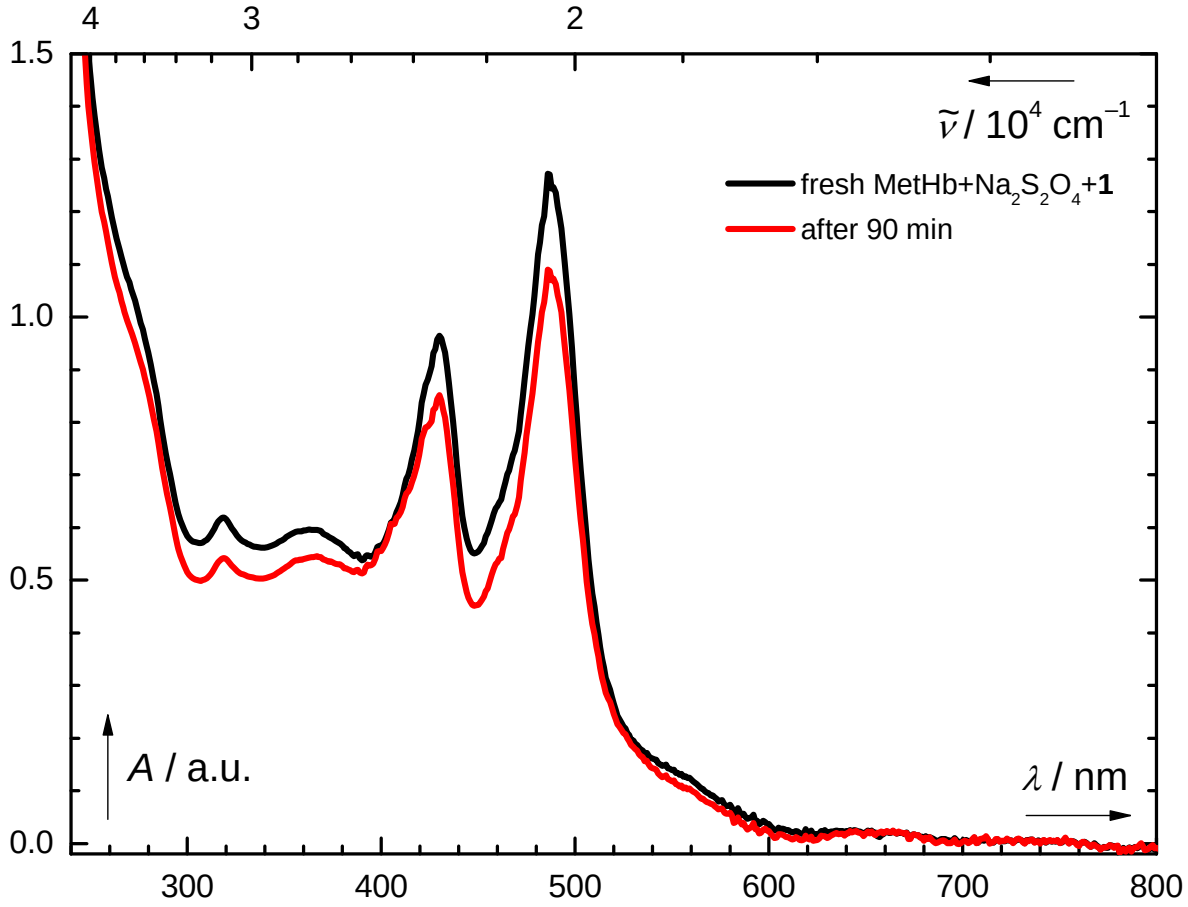

Figure S20. UV-vis (aq phosphate buffer, $I \sim 0.1$ M, pH = 7.4): Hb, HbO_2, HbCO and a mixture of Hb and **1** (aq phosphate buffer, $I \sim 0.1$ M, pH = 7.4, aerated) irradiated at $\lambda = 503 \pm 15$ nm to ~50% conversion (a remaining amount of **1** is detectable at $\lambda_{max} = 489$ nm); total irradiation time 4.6 h; for more details see page S4.

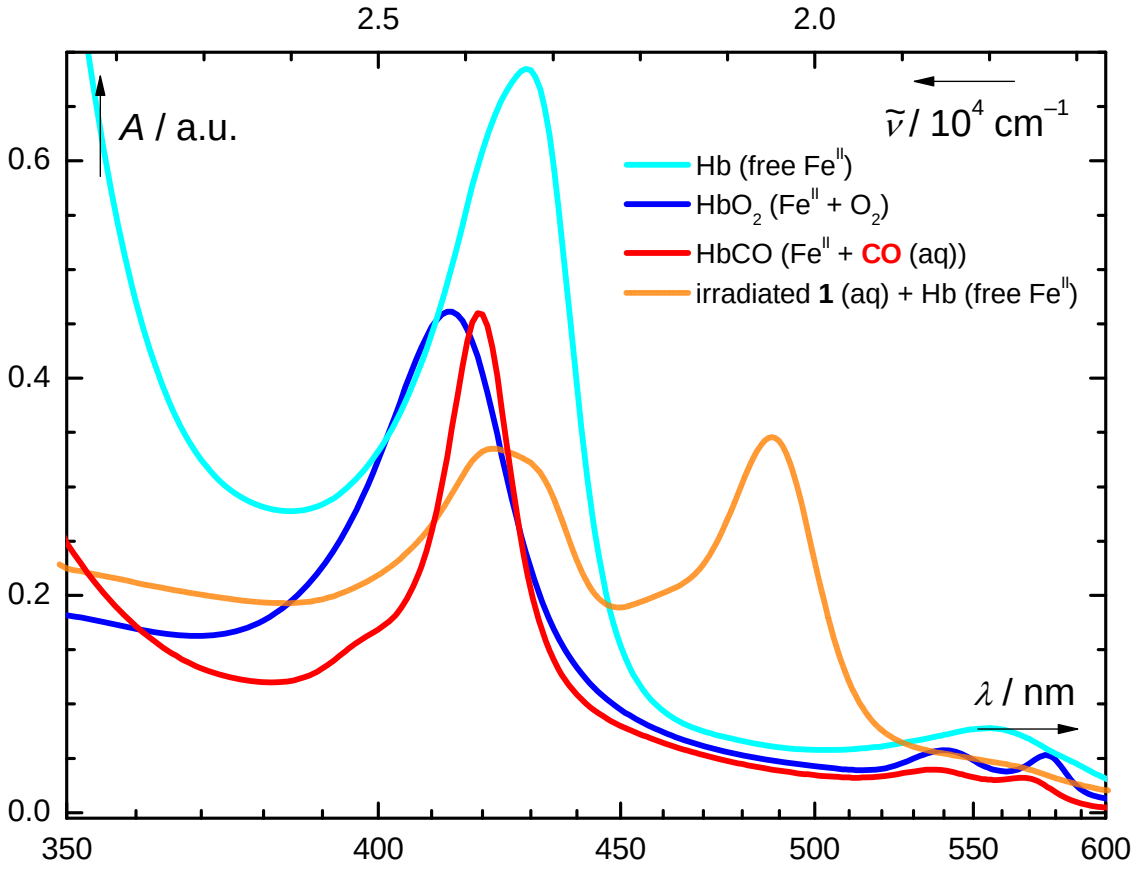

Figure S21. UV-vis (aq phosphate buffer, $I \sim 0.1$ M, pH = 9.5, aerated): **1** (black line: fresh solution; red line: solution irradiated for 2 days at λ = 503 ± 15 nm)

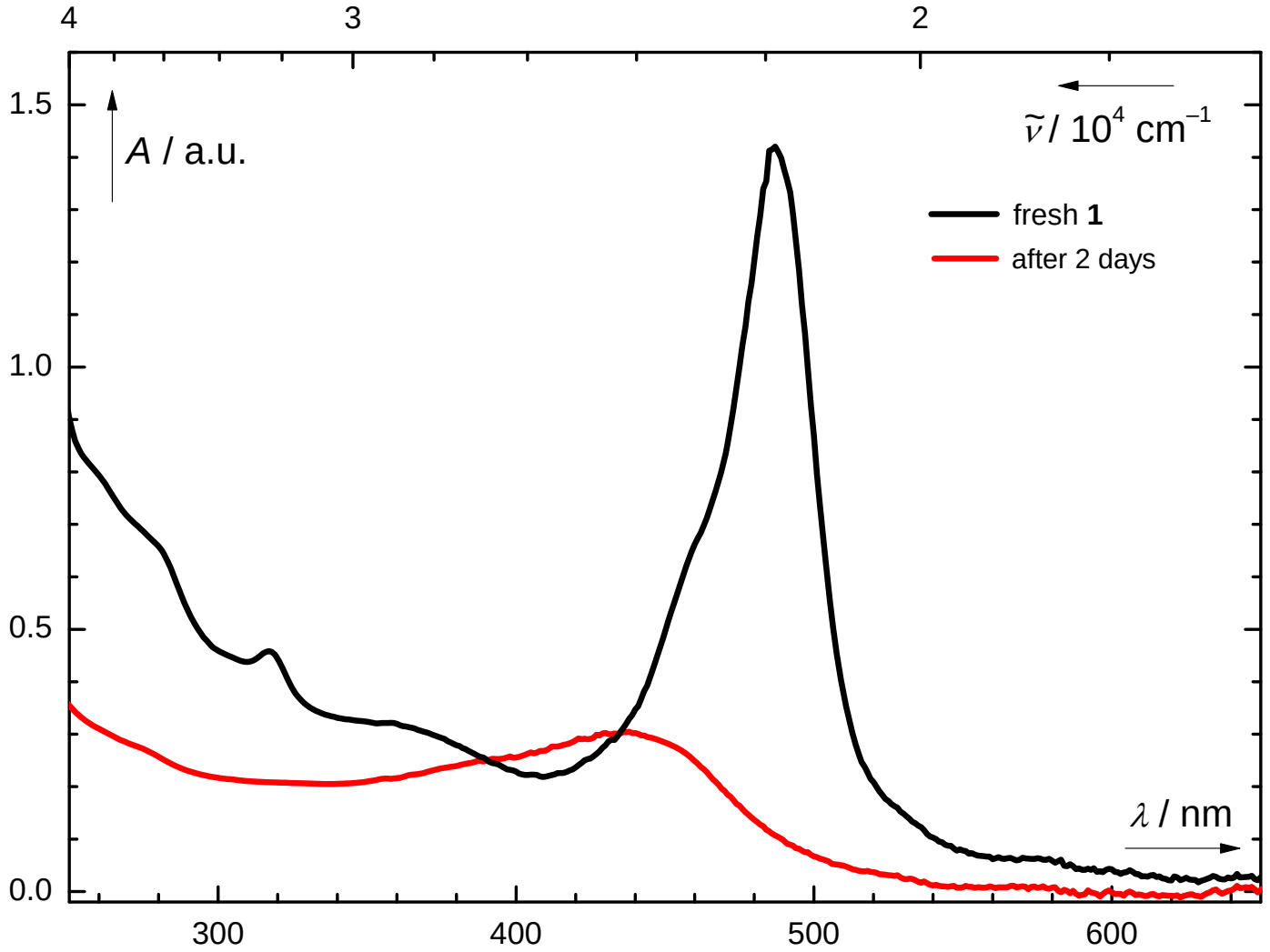

Figure S22. HRMS (ES+): 3,6-Dihydroxy-9*H*-xanthen-9-one (**3**)

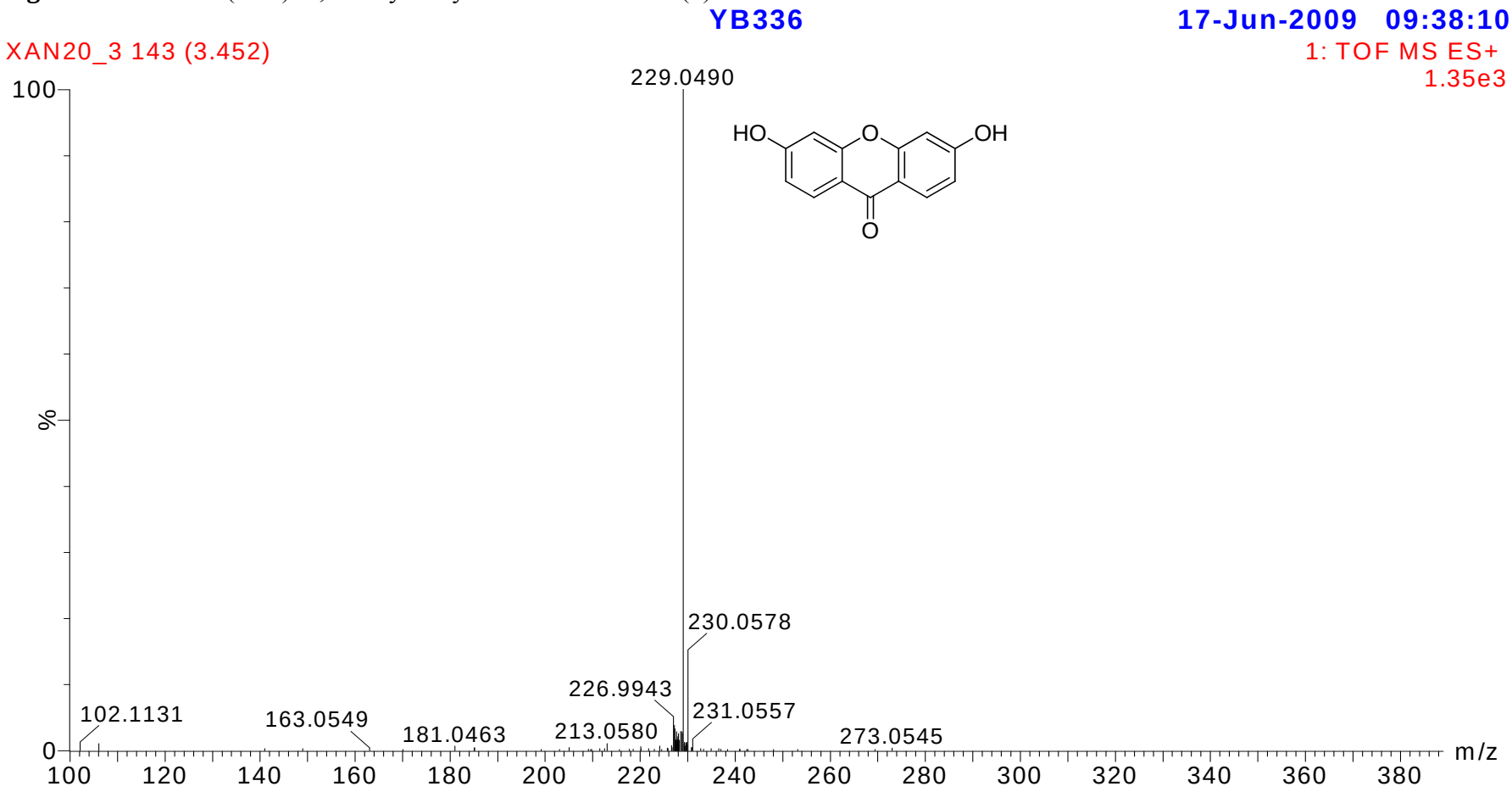

calcd for $C_{13}H_9O_4$ [M + H^+] 229.0495

Figure S23. HRMS (ES+): 3,6-Dihydroxy-9*H*-xanthen-9-one (**3**)

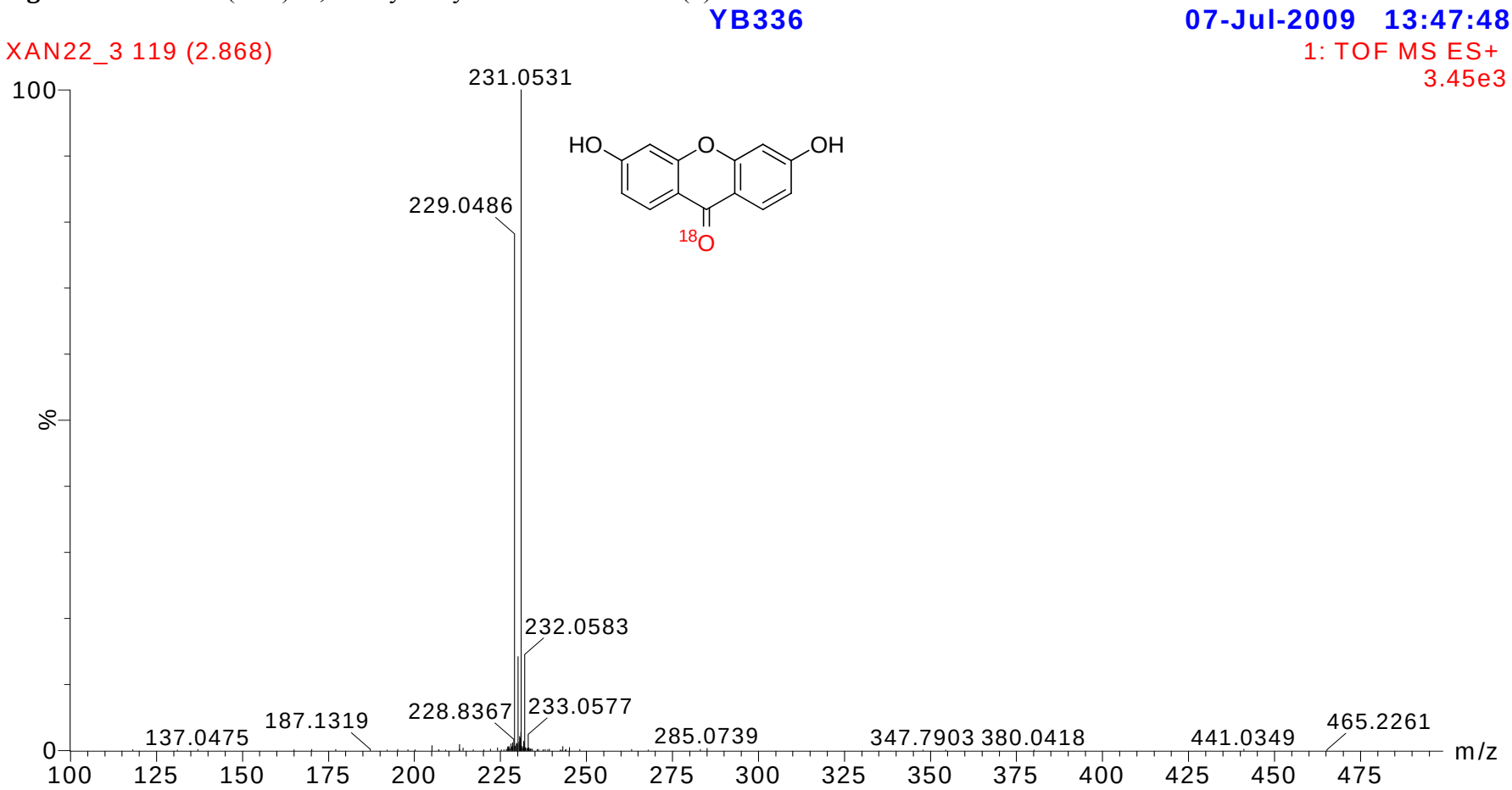

calcd for $C_{13}H_9{}^{16}O_3{}^{18}O$ [M + H^+] 231.0538

Figure S24. Differential thermal scanning calorimetry (DSC, blue line) and thermogravimetric analysis (TG, green line) with coupled IR analysis (Gram Schmidt, black line; it represents vectorial sum of the intensity in the entire IR spectra) of the released gases: 6-Hydroxy-3-oxo-3*H*-xanthene-9-carboxylic acid (**1**)

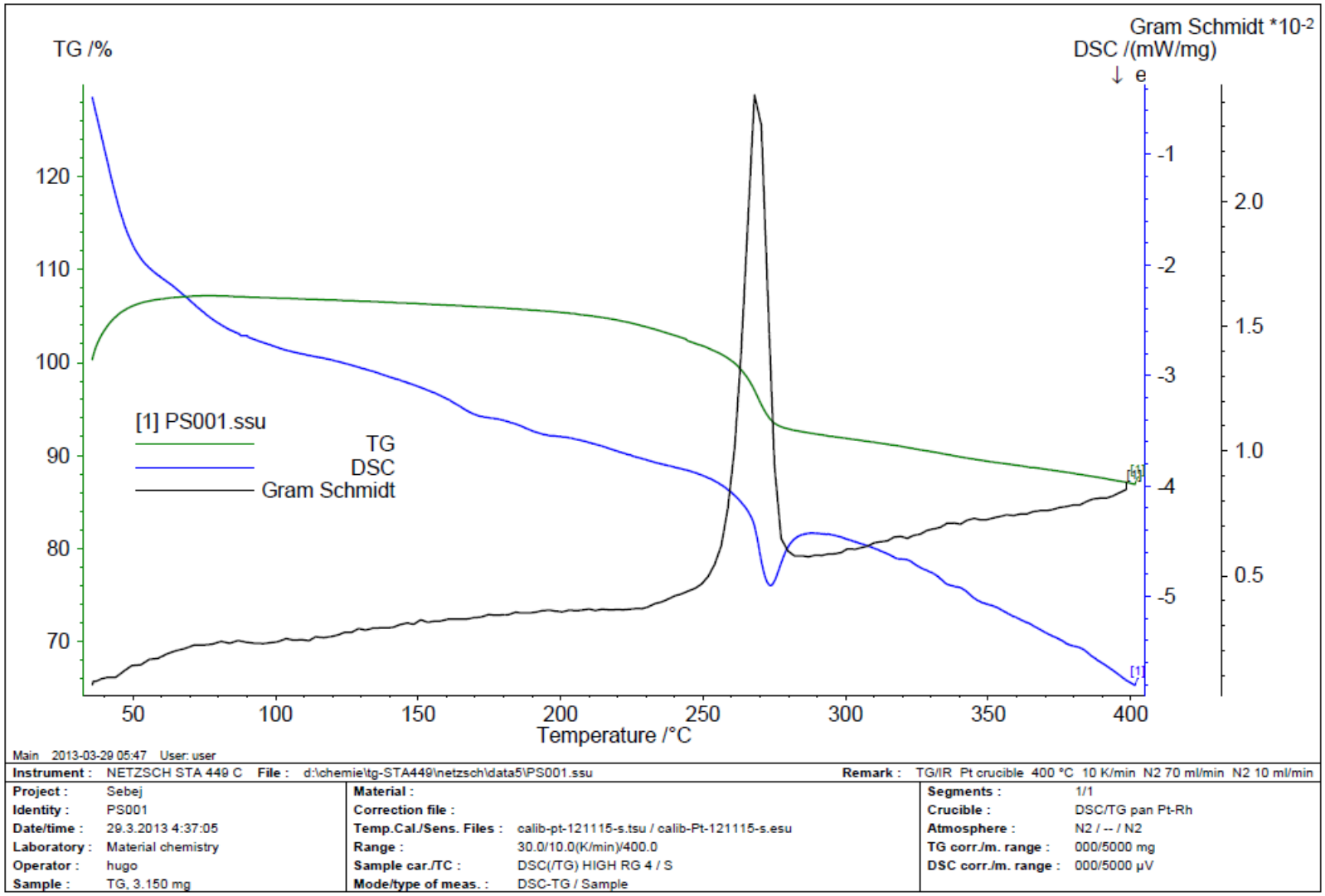

Figure S25. IR of the gases released (the spectrum was recorded at the maximum intensity observed at 2359 cm^{-1}) during the thermal scanning calorimetry and thermogravimetric analysis: 6-Hydroxy-3-oxo-3*H*-xanthene-9-carboxylic acid (**1**)

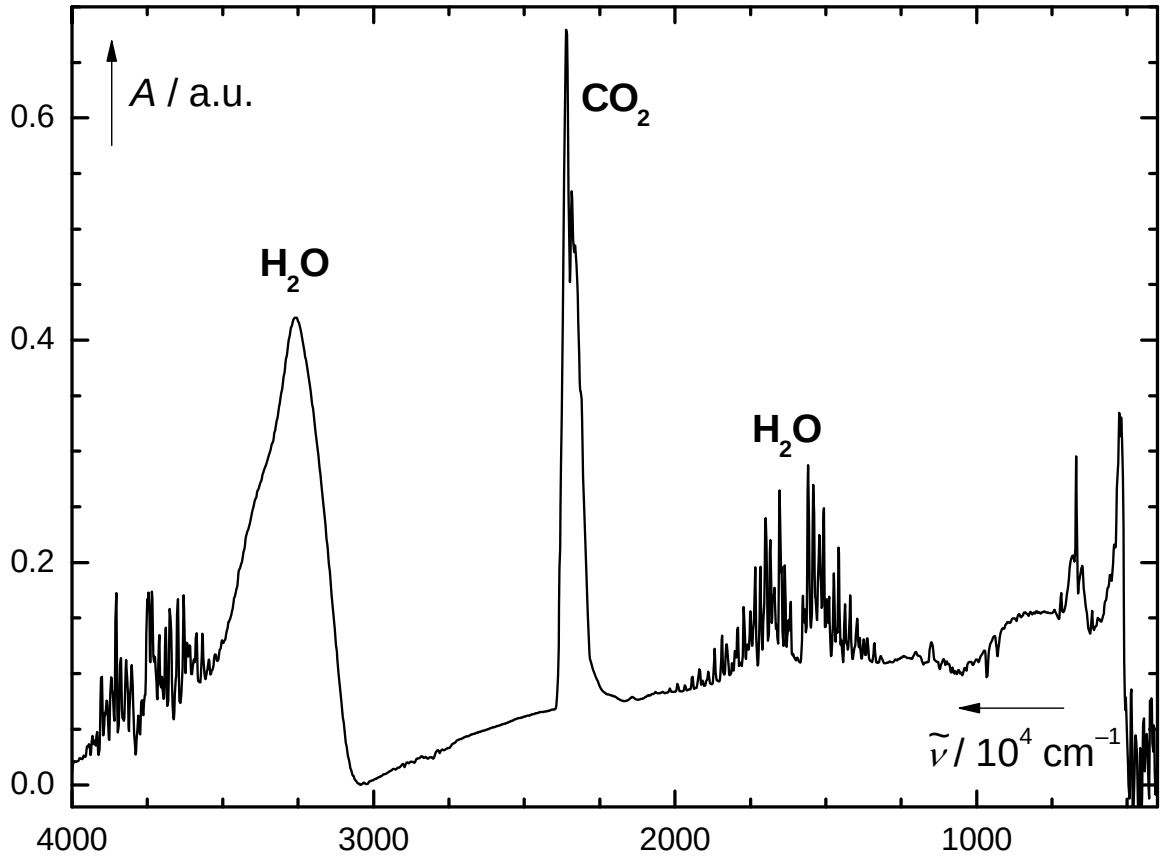

Various non-photochemical synthetic strategies to obtain **1** were tested.

1. Nucleophilic attack to the C-9 carbon of **3** and its derivatives, e.g.:

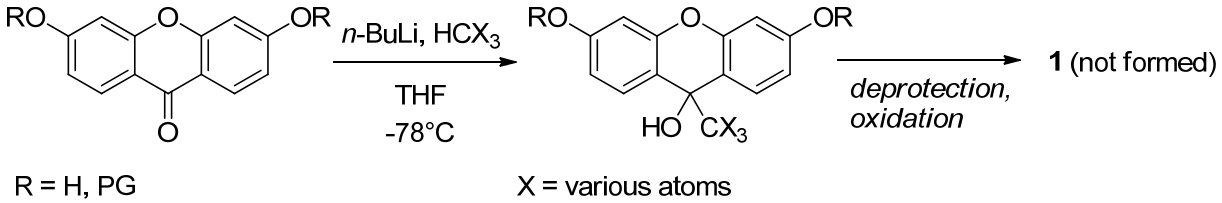

2. Oxidation of C-sp3 carbon at C-9 of **2** and its derivatives, e.g.:

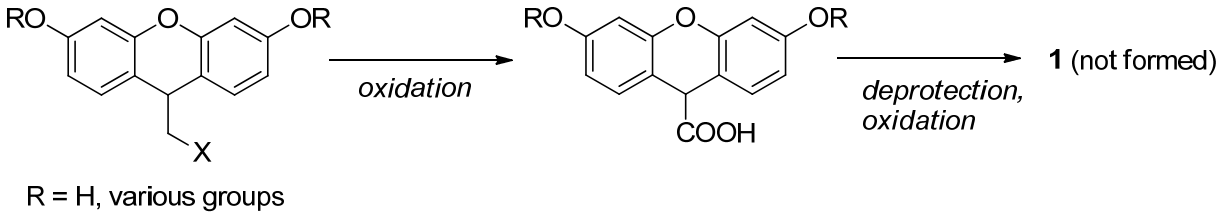

3. Condensation of resorcinol with various reagents containing CR_3-COOH synthon, similar to that described in reference 11 of the main text and references therein.
4. The hydrolysis of a 9-cyano derivative:

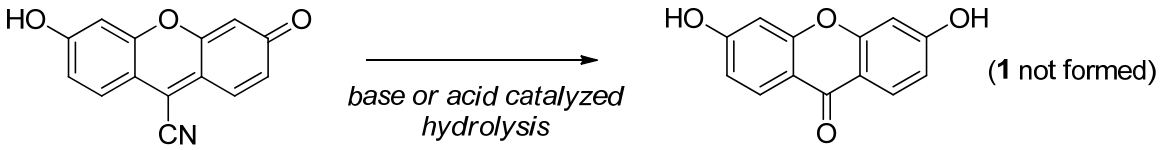

Scheme S2. Unsuccessful syntheses of **1**.

References

(1) Gottlieb, H. E.; Kotlyar, V.; Nudelman, A., *J. Org. Chem.* **1997,** *62*, 7512.
(2) Frisch, M. J.; Trucks, G. W.; Schlegel, H. B.; Scuseria, G. E.; Robb, M. A.; Cheeseman, J. R.; Scalmani, G.; Barone, V.; Mennucci, B.; Petersson, G. A.; Nakatsuji, H.; Caricato, M.; Li, X.; Hratchian, H. P.; Izmaylov, A. F.; Bloino, J.; Zheng, G.; Sonnenberg, J. L.; Hada, M.; Ehara, M.; Toyota, K.; Fukuda, R.; Hasegawa, J.; Ishida, M.; Nakajima, T.; Honda, Y.; Kitao, O.; Nakai, H.; Vreven, T.; Montgomery, J., J. A. ; Peralta, J. E.; Ogliaro, F.; Bearpark, M.; Heyd, J. J.; E. Brothers; Kudin, K. N.; Staroverov, V. N.; Kobayashi, R.; Normand, J.; Raghavachari, K.; Rendell, A.; Burant, J. C.; Iyengar, S. S.; Tomasi, J.; Cossi, M.; Rega, N.; Millam, J. M.; Klene, M.; Knox, J. E.; Cross, J. B.; Bakken, V.; Adamo, C.; Jaramillo, J.; Gomperts, R.; Stratmann, R. E.; Yazyev, O.; Austin, A. J.; Cammi, R.; Pomelli, C.; Ochterski, J. W.; Martin, R. L.; Morokuma, K.; Zakrzewski, V. G.; Voth, G. A.; Salvador, P.; Dannenberg, J. J.; Dapprich, S.; Daniels, A. D.; Farkas, Ö.; Foresman, J. B.; Ortiz, J. V.; Cioslowski, J.; Fox, D. J. *Gaussian 09, Revision A.1*, Gaussian, Inc.,: Wallingford, CT, 2009.
(3) Boese, A. D.; Martin, J. M. L., *J. Chem. Phys.* **2004,** *121*, 3405.
(4) Peach, M. J. G.; Helgaker, T.; Salek, P.; Keal, T. W.; Lutnaes, O. B.; Tozer, D. J.; Handy, N. C., *Phys. Chem. Chem. Phys.* **2006,** *8*, 558.
(5) Zhao, Y.; Truhlar, D. G., *Acc. Chem. Res.* **2008,** *41*, 157.
(6) Šebej, P.; Wintner, J.; Müller, P.; Slanina, T.; Al Anshori, J.; Antony, L. A. P.; Klán, P.; Wirz, J., *J. Org. Chem.* **2013,** *78*, 1833.
(7) Zijlstra, W. G.; Buursma, A., *Comp. Biochem. Phys. B* **1997,** *118*, 743.
(8) Ouchi, A.; Obata, T.; Oishi, T.; Sakai, H.; Hayashi, T.; Ando, W.; Ito, J., *Green Chem.* **2004,** *6*, 198.
(9) Creutz, C.; Sutin, N., *Inorg. Chem.* **1974,** *13*, 2041.